Annual Report

Authors

Peter Rudling
ANT International, Mölnlycke, Sweden

Alfred Strasser
Sleepy Hollow, NY, USA

Friedrich Garzarolli
Fürth, Germany

Kit Coleman
Ontario, Canada

Charles Patterson
Clovis, CA, USA

A.N.T. INTERNATIONAL®

© December 2014
Advanced Nuclear Technology International
Analysvägen 5, SE-435 33 Mölnlycke
Sweden

info@antinternational.com
www.antinternational.com

Disclaimer

The information presented in this report has been compiled and analysed by Advanced Nuclear Technology International Europe AB (ANT International®) and its subcontractors. ANT International has exercised due diligence in this work, but does not warrant the accuracy or completeness of the information. ANT International does not assume any responsibility for any consequences as a result of the use of the information for any party, except a warranty for reasonable technical skill, which is limited to the amount paid for this assignment by each Project programme member.

Copyright © Advanced Nuclear Technology International Europe AB, ANT International, 2014.

Contents

1 Introduction (Peter Rudling) 1-1

2 Burnup achievements and key fuel performance (Alfred Strasser) 2-1

2.1 Introduction 2-1

2.2 Trends in fuel operating conditions 2-1

2.2.1 General trends 2-1

2.2.2 Fuel cycles 2-2

2.2.3 Power uprates 2-4

2.2.4 Burnup extension 2-5

2.3 Fuel reliability 2-7

2.3.1 Overall failure rates 2-7

2.4 High burnup UO_2 and MOX fuel performance 2-11

2.4.1 Thermal conductivity 2-11

2.4.2 Effect of irradiation on structure 2-14

2.4.3 Effect of additives 2-15

2.4.4 Fission gas behaviour 2-20

2.5 High burnup performance of zirconium alloys 2-35

2.5.1 Cladding Oxidation 2-35

2.5.2 Hydride characterization 2-47

2.5.3 Hydride orientation 2-52

2.5.4 Effect of hydrogen on mechanical properties 2-64

2.6 BWR water chemistry 2-70

2.6.1 Hydrogen Water Chemistry (HWC) 2-70

2.6.2 On-Line Noble Metal Chemistry (OLNC) 2-71

2.6.3 Crud deposition 2-79

3 Microstructure and manufacturing (Friedrich Garzarolli) 3-1

3.1 Introduction 3-1

3.2 New results on texture and anisotropy 3-3

3.3 New results on irradiant induced microstructural changes 3-11

3.4 New results on the solubility and equilibrium concentrations differences 3-23

3.5 Summary Microstructure 3-27

4 Mechanical properties (Kit Coleman) 4-1

4.1 Introduction 4-1

4.2 Situations for potential damage to fuel 4-1

4.2.1 Contact 4-1

4.2.2 Pellet-clad-interaction (PCI) 4-11

4.2.3 Hydrogen effects. 4-17

4.3 Fatigue 4-47

4.4 Miscellaneous potential hazards and observations 4-50

4.5 Water Reactor Fuel Performance Meeting 2014, Sendai, Japan. 4-50

4.5.1 Fukushima 4-51

4.5.2 Cleaning the site 4-53

4.5.3 Lessons learnt. 4-54

4.6 Summary 4-55

5 Dimensional stability – Charged particle bombardment of Zr alloys (Ron Adamson) 5-1

6 Corrosion and hydriding (Friedrich Garzarolli) 6-1

Copyright © Advanced Nuclear Technology International Europe AB, ANT International, 2014.

6.1 Overview on nodular corrosion 6-1
6.1.1 Introduction 6-1
6.1.2 Growth of nodular oxide 6-3
6.1.3 Parameters impacting nodular corrosion tendency 6-8
6.1.4 Oxide measurement technique 6-28
6.1.5 Potential consequences 6-29
6.1.6 Hydrogen pickup 6-30
6.1.7 Nodular corrosion mechanisms 6-31
6.2 General overview on shadow corrosion 6-35
6.2.1 Introduction 6-35
6.2.2 Appearance 6-35
6.2.3 Reported peak shadow corrosion 6-44
6.2.4 Potential consequences of shadow corrosion 6-54
6.2.5 Evaluation of data on hydrogen pickup 6-54
6.2.6 Critical conditions for shadow corrosion 6-56
6.2.7 Mechanism 6-62
6.3 Out reactor corrosion 6-69
6.3.1 Recent publications on the corrosion mechanism 6-69
6.3.2 Recent publications on out reactor corrosion 6-84
6.4 In reactor corrosion 6-89
6.4.1 Corrosion in PWR and PHWRs 6-89
6.4.2 In-BWR corrosion 6-93
6.5 Summary 6-97
7 Primary failure and secondary degradation – open literature data (Peter Rudling) 7-1
7.1 Introduction 7-1
7.1.1 Primary failures 7-1
7.1.2 Secondary degradation 7-5
7.2 Results presented in year 2014-2015 7-5
7.2.1 Primary fuel failure causes 7-5
7.3 Summary and highlights – year 2013-2014 7-34
8 Cladding performance under accident conditions LOCA and RIA (Peter Rudling) 8-1
8.1 Introduction 8-1
8.1.1 Loss of Coolant Accident 8-1
8.1.2 Reactivity initiated accident 8-6
8.2 New results 8-13
8.2.1 RIA 8-13
8.3 LOCA 8-28
8.3.1 Ballooning and burst 8-28
8.3.2 Oxidation and Hydrogen Pickup 8-32
8.3.3 TFGR during LOCA 8-43
8.3.4 Post Quenched Ductility (PQD) by Ring Compression Tests (RCTs) 8-46
8.3.5 Integral testing 8-53
8.3.6 Fuel dispersal 8-55
8.3.7 Modelling 8-65
8.3.8 Performance of new LOCA oxidation resistant materials 8-70
8.4 Severe Accidents 8-72
8.4.1 Hydrogen desorption 8-73
8.5 Summary of recent key results 2013-2014 8-73

Copyright © Advanced Nuclear Technology International Europe AB, ANT International, 2014.

9 Dry Storage (Charles Patterson) 9-1
9.1 Introduction 9-1
9.2 Status of interim storage programs 9-9
9.2.1 U.S.A. 9-9
9.2.2 International 9-14
9.3 Dry storage conditions relevant to fuel performance 9-17
9.4 Extended storage 9-18
9.5 Waste form 9-20
9.6 Nuclear safety 9-21
9.7 Drying and residual moisture 9-24
9.7.1 Vacuum drying 9-25
9.7.2 Residual moisture 9-26
9.7.3 Ice formation during vacuum drying 9-27
9.7.4 Breached fuel rods 9-28
9.7.5 Bound water 9-28
9.7.6 Radiolysis 9-29
9.7.7 Assessment of drying adequacy 9-42
9.8 Temperature and heat transfer 9-43
9.9 Cladding stress 9-49
9.10 Hydrogen and hydriding 9-54
9.11 Storage and transportation accidents 9-64
10 Dysprosium Hafnate – A new absorber (Alfred Strasser) 10-1
10.1 Introduction 10-1
10.2 Transmutations and nuclear properties 10-2
10.3 Properties 10-7
10.3.1 Phase diagram 10-7
10.3.2 Physical Properties 10-7
10.3.3 Mechanical Properties 10-11
10.4 Fabrication 10-12
10.5 Irradiation testing 10-14
10.6 Summary 10-18
11 Trends and needs 11-1
12 References 12-1
Nomenclature
Unit conversion

Copyright © Advanced Nuclear Technology International Europe AB, ANT International, 2014.

1 Introduction (Peter Rudling)

The objective of the Annual Review of ZIRconium Alloy Technology (ZIRAT) and Information on Zirconium Alloys (IZNA) is to review and evaluate the latest developments in ZIRAT as they apply to nuclear fuel design and performance.

The objective is met through a review and evaluation of the most recent data on zirconium alloys and to identify the most important new information and discuss its significance in relation to fuel performance now and in the future. Included in the review are topics on materials research and development, fabrication, component design, and in-reactor performance presented in conferences, journals and reports.

The primary issues addressed in the review and this report is zirconium alloy research and development, fabrication, component design, ex- and in-reactor performance including:

- Regulatory bodies and utility perspectives related to fuel performance issues, fuel vendor developments of new fuel design to meet the fuel performance issues.
- Fabrication and Quality Control (QC) of zirconium manufacturing, zirconium alloy systems.
- Mechanical properties and their test methods (that are not covered in any other section in the report).
- Dimensional stability (growth and creep).
- Primary coolant chemistry and its effect on zirconium alloy component performance.
- Corrosion and hydriding mechanisms and performance of commercial alloys.
- Cladding primary failures.
- Post-failure degradation of failed fuel.
- Cladding performance in postulated accidents (Loss of Coolant Accident (LOCA), Reactivity Initiated Accident (RIA)).
- Dry storage.
- Potential Burn-up (BU) limitations.
- Current uncertainties and issues needing solution are identified throughout the report.

Background data from prior periods have been included wherever needed. The data published in this Report is only from non-proprietary sources; however, their compilation, evaluations, and conclusions in the report are proprietary to ANT International and ZIRAT/IZNA members as noted on the title page.

The authors of the report are Mr. Friedrich Garzarolli, Mr. Alfred Strasser, Dr. Charles Patterson, Dr. Christopher Coleman and Mr. Peter Rudling, President of ANT International.

The work reported herein will be presented in two Seminars: in Clearwater Beach, FL., USA (February 9-11, 2014) and in Palma de Mallorca, Spain (March 9-11, 2014).

The Term of ZIRAT19/IZNA14 started on February 1, 2014 and ends on March 31, 2015.

All literature that we refer to in this Report is available in the ANT International Literature Database (LDB). Please contact Ms. Angela Olpretean at angela.olpretean@antinternational.com for more information.

Copyright © Advanced Nuclear Technology International Europe AB, ANT International, 2014.

2 Burnup achievements and key fuel performance (Alfred Strasser)

2.1 Introduction

The objective of this Section is to summarize the key performance issues that could affect fuel design, fabrication or operation of the nuclear fuel in the near term or the longer term. Topics covered include the fuel itself and all the fuel assembly components made of zirconium alloys nickel base alloys and stainless steels. The information sources reviewed, screened and evaluated include nearly all the related publications and technical meeting presentations of the past, approximately 18 months and focuses primarily on **extended burnup** data. The Section is intended to be a guide to significant, current issues and provide an alert to items that could affect fuel related operations. The extensive volume of information involved limits the presentations to the most significant features and conclusions, and the reader is urged to refer to the referenced publications for more detail.

2.2 Trends in fuel operating conditions

2.2.1 General trends

Improved fuel reliability and operating economics are the driving forces for the changes in operating conditions, while maintaining acceptable margins to operating and regulatory safety limits. These are incentives for significant advances in materials technology, software for designing and predicting fuel performance, sophisticated instrumentation, modifications in water chemistry and methods for post-irradiation examinations. Some of these advances in technology have increased the demands on fuel performance levels and put pressure on the regulatory bodies to license operations to increased burnup levels. The types of changes in LWR operating methods intended to achieve improved safety and economics have not changed in the past years and still include:

- Annual fuel cycles extended to 18 and 24 months,
- Increased discharge burnups as high as 64 GWDf/MT batch average exposures by higher enrichments, increased number of burnable absorbers in the assemblies and in PWRs higher Li and B levels in the coolant, or enriched B in the coolant,
- Plant power uprates that range from 2 to 20%,
- More aggressive fuel management methods with increased enrichment levels and peaking factors,
- Reduced activity transport by Zn injection into the coolant,
- Improved water chemistry controls and increased monitoring,
- Component life extension with hydrogen water chemistry (HWC), noble metal chemistry (NMC) and on-line noble metal chemistry (OLNC) in BWRs.

Copyright © Advanced Nuclear Technology International Europe AB, ANT International, 2014.

2.2.2 Fuel cycles

Cycle Lengths

The trend for increased fuel cycle lengths has come to a near "equilibrium" in the US with PWRs operating at an average of 500 effective full power days (EFFPD) per cycle and BWRs an average of 620 EFFPD per cycle, up to a maximum of about 680 days for PWRs and 720 days for BWRs . Nearly all the US BWRs are trending toward 24 month cycles. The older, lower power density PWRs have implemented the 24 month cycles, but fuel management limitations, specifically the reload batch sizes required, have limited implementation of 24 month cycles in the high power density plants. The economics of 24 month cycles tend to become plant specific since they depend on the balance of a variety of plant specific parameters. The potential economic gains for cycle extension have decreased in the US as the downtimes for reloading and maintenance procedures have been significantly reduced, increasing the capacity factors.

Most countries outside the US have one, winter power peak annually compared to the two, winter and summer peaks in the US, and this has tended to keep them on annual cycles. Changes in load management, economics, maintenance practices and licensing procedures have tended to change this and some countries, such as France, Belgium, Switzerland and Germany have applied both annual and 18 month cycles.

Capacity Factors

The capacity factors of US plants has been tracked for 3 year periods starting with 1975-1977 until most recently for 2011-2013 [Blake, 2014]. The number of plants covered in 2011-2013 has been reduced from 104 to 100, to account for plants that have been permanently shut down. The median capacity of the plants has been quite constant, close to 90%, ever since the period of 2002 to 2010. The mean factors for the BWRs and PWRs have been nearly identical varying less than 1% differential (Figure 2-1). The spread between the top and bottom quartile plants as a function of years is given in Figure 2-2 and shows that the top quartile has been above 92% consistently since the 1999-2001 period and the bottom quartile has improved except for a slip in the most recent period, due to the shutdown of some of the plants. It is of interest to note that the median factor of 89.73% of multi-unit sites is higher than the 85.69% factor for single unit sites in the 2011-2013 period.

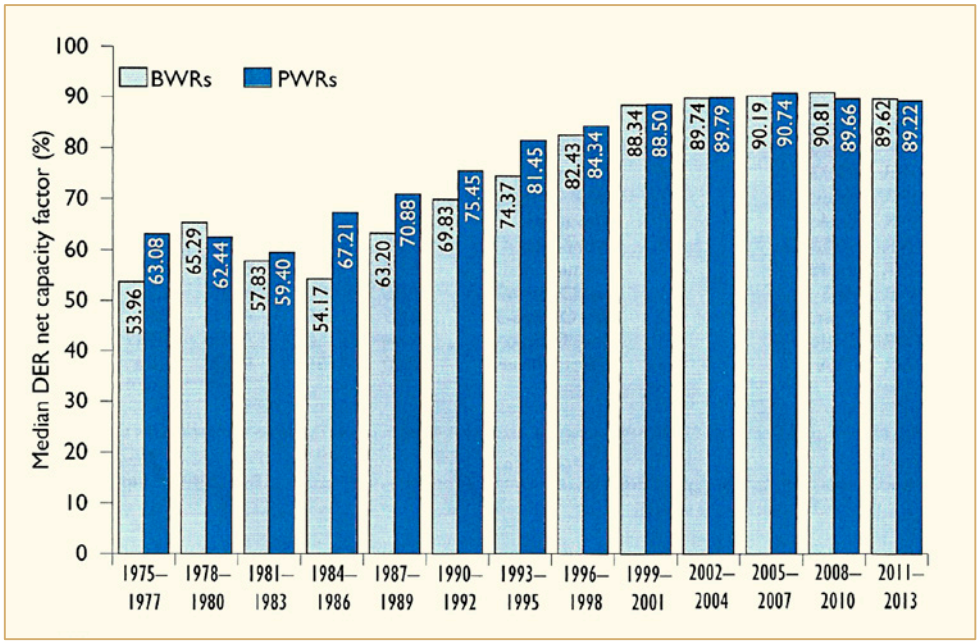

Figure 2-1: US plant capacity factor history [public information INPO/WANO 2014].

Copyright © Advanced Nuclear Technology International Europe AB, ANT International, 2014.

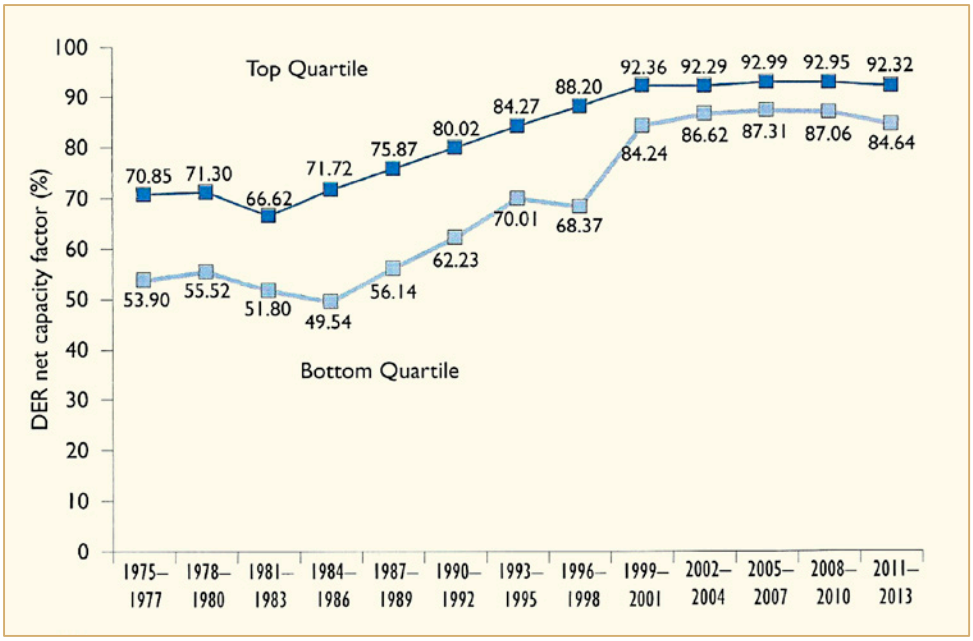

Figure 2-2: US plant top and bottom quartile capacity factors [public information INPO/WANO 2014].

Operational requirements may not require the highest capacity factor for the most economical operation; load following is a typical example. Plant performance ratings should therefore be extended beyond their capacity factors and include items such as the forced loss rate, the safety system and industrial safety performance, the scram trend, radiation exposure and other factors tracked by the Institute of Nuclear Power Operations (INPO) and World Association of Nuclear Operators (WANO). The trends through 2013 for some of these factors show general improvements over the years that exceed the goals in some cases (Figure 2-3).

Copyright © Advanced Nuclear Technology International Europe AB, ANT International, 2014.

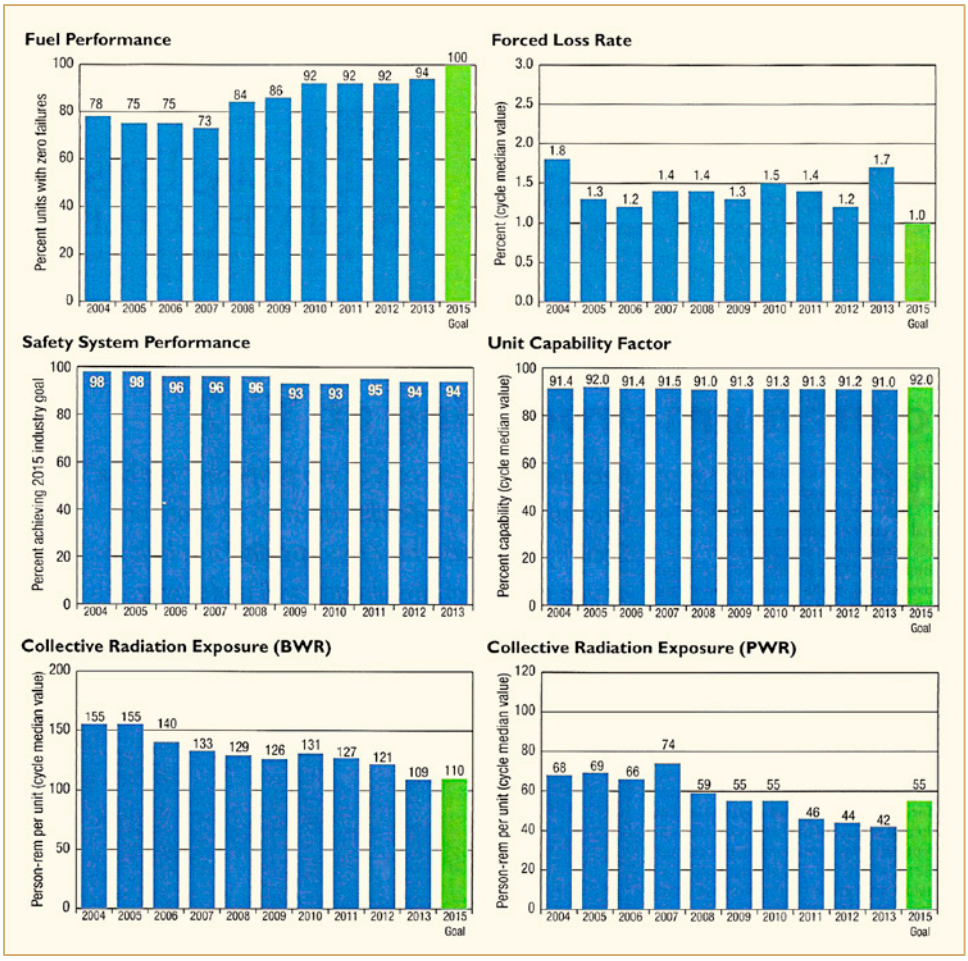

Figure 2-3: US plant performance factor trends [public information INPO/WANO 2014].

2.2.3 Power uprates

The power of the majority of the US operating plants has been uprated, by a maximum of 20%. While the fuel performance limits remain the same for the uprated conditions, the number of fuel assemblies operating at higher power change and the margin to the limits might be reduced. The effect of higher flow rates on hydraulic and water chemistry effects and their interaction with the fuel must also be considered. These changes have not affected the failure rate or apparently the fuel performance; however, it does increase the statistical probability of the effects of increasing power and burnup related factors on the fuel performance.

Copyright © Advanced Nuclear Technology International Europe AB, ANT International, 2014.

The power uprates approved in the US since 2011 are in % MWth:

BWRs:		PWRs:	
Limerick 1 & 2	1.65% each	Harris	1.6%
LaSalle 1 & 2	1.65% each	Braidwood 1 & 2	1.6% each
Nine Mile Point 2	15.0%	Byron 1 & 2	1.6% each
Fermi 2	1.6%	McGuire 1 & 2	1.7% each
Grand Gulf 1	13.1%	St. Lucie 1 & 2	11.9% each
Monticello	12.9%2	Turkey Point 3 & 4	15.0% each
Peach Bottom 2 & 3	12.4% each	Point Beach 1 & 2	17.0% each

Power uprate applications under review are:

	PWR:
Oconee 1, 2 & 3	1.6% each
Catawba 1	1.7%

The net gain of the uprating is about 620 MWe, which does not balance the 3,534 MWe lost due to the shutdown of reactors, decreasing the overall nuclear generation in the US. Power uprating is of course practiced outside the US as well.

The effect of power uprating on power distribution among the fuel assemblies was discussed in ZIRAT12/IZNA7 Annual Report [Strasser et al, 2007] and the effect on water chemistry was discussed in the LCC3 Special Topic Report "Consequences of Power Uprating" [Lundgren & Riess, 2007] in the LCC3 Seminar.

2.2.4 Burnup extension

The major incentive for extended burnups is the potentially improved fuel cycle economy. Economic analyses in past ZIRAT/IZNA reports indicated that economic incentives for extending burnups beyond the 60-70 GWD/MT batch average range will disappear and that other incentives must exist in order to justify going beyond the economically optimal level. The improved economics depend in part on the decreased amount of spent fuel assemblies to be purchased, handled and disposed of. This is balanced by the increased amount of uranium and enrichment services required. The economics of decreased assemblies could also be impacted by the much longer cooling times required for high burnup and MOX fuels in spent fuel pools prior to on-site dry storage or transport to a storage facility as noted later, impacting the spent fuel pool capacities. The economic analyses are also dependent on the utility's accounting systems and as a result are utility and even plant specific.

The burnup limits are established by the regulatory agencies in each country based primarily on the thermo-mechanical performance of the fuel under normal and accident conditions as well as unintended self-imposed limits of specific designs that are below the regulatory limits. The many factors that affect and support these limits are discussed throughout the extensive ZIRAT/IZNA reports.

Copyright © Advanced Nuclear Technology International Europe AB, ANT International, 2014.

In addition to the thermal-mechanical limits is the additional limit of <5% peak enrichment observed internationally. Enrichments above this limit could increase burnup, reduce batch sizes and improve fuel cycle efficiency. The effect of such designs have been evaluated and indicate that fuel cycle designs with greater enrichments may not meet thermal limits and would add uncertainties and requirements for relicensing adding costs in addition to relicensing the equipment and mechanics of handling the fuel at the fabrication plant and reactor site. The results of some studies were given in the ZIRAT16/IZNA11 Annual Report [Adamson et al, 2011].

The average batch burnups in US PWRs are currently in the range of 43-58 GWD/MT and in US BWRs in the range of 43-52 GWD/MT. The PWR burnups have levelled off and the BWRs are still increasing slightly, approaching the NRC regulatory limit of 62.5 GWD/MT peak rod. The NRC does not have any current activities to evaluate the potential increase of this limit, so that the burnups will plateau at these levels at this time.

In Europe, the batch average burnup in Switzerland has been as high as 65 GWD/MT with concurrent assembly and rod burnups of 68 and 73 GWD/MT burnups respectively. This has been possible, in part, due to the greater margin to regulatory limits in some countries. The burnup ranges by countries are compared to their regulatory limits in Table 2-1.

Table 2-1: Maximum bus achieved vs. regulatory limits, (excludes LTAs).

	BU (GWD/MT)				
Country	**Batch**	**Assembly**	**Rod**	**Pellet**	**Regulatory Limit**
USA	57	58	62	73	62.5 peak rod
Belgium		50-55			55 UO_2 assy., 50 MOX assy.
Czech Republic	51	56	61		60 peak rod
Finland	45.6*	48.6	58		57 assy. (for PWR)
France	47	51 UO_2 42 MOX			52 assy.
Germany	58	62	68		65 assy.
Hungary		50	62		
Japan	50	55	62		55 UO_2 assy., 45 MOX assy.
Korean Republic	46				60 rod
Netherlands	52	55	59		60 rod
Russia	60	65			
Spain	50.4	57.4	61.7	69	
Sweden	47	57.2	63.6	65	60 assy., 64 rod
Switzerland	64	68	73		80 pellet
Taiwan					60 rod (P), 54 assy. (B)
UK	44.3	46.5	50		55 pellet
Ukraine		50			

*Current batch design for 50 GWD/MT in BWR

ANT International, 2014

Copyright © Advanced Nuclear Technology International Europe AB, ANT International, 2014.

The Ringhals plants in Sweden have plans to target >65 GWD/MT assembly burnups with the Westinghouse Next Generation Fuel (NGF) [Chapin et al, 2013]. Westinghouse has developed the PAD5 version of their fuel performance code based on input data from the irradiation of 8 rods to 70 GWD/MT and 30 rods to 75 GWD/MT [Long et al, 2013]. The Russians have a goal to reach 70-80 GWD/MT assembly burnup with the fuel in their advanced VVER 1200 plant [Ivanova et al, 2013].

The lead test assemblies (LTAs) used to test new design concepts and materials are licensed to higher burnups than the reload batches for power production. Fuel rod burnups of close to 100 GWD/MT have been achieved by past PWR LTAs. Some of the LTAs and their currently achieved burnups are listed in Table 2-2. Their goal burnups are not available.

Table 2-2: Exposure status of some LTAs as of the fall, 2014.

Reactor	LTA design	GWD/MT
BWR	ATRIUM 10XM	20, 43, 54
	ATRIUM 11/LTP2	14
	GNF2/P8	39
	GNF2/P9	49
	SVEA96, Optima 3/LK3	15, 43
	ZIRLO Channels	46, 60
PWR	Agora 4H (HTP)	27
	AREVA 15×15-20/M5	16
		ANT International, 2014

Approximate equivalence of burnup to neutron exposures can be given as 50 GWD/MT to about 1×10^{22} n/cm^2 (>1 MeV) or 17 dpa; however, this relationship depends on several factors such as enrichment, extent of moderation and neutron energy spectrum and should be evaluated for each specific case.

2.3 Fuel reliability

2.3.1 Overall failure rates

The industry goal of zero fuel failures in the US has been approached, but has levelled off at about 96% of the plants operating without failed fuel (Figure 2-4). As of May, 2014 there were only 4 plants operating in the US with failed fuel as noted on the Figure, of which 3 were BWRs and one a PWR.

Copyright © Advanced Nuclear Technology International Europe AB, ANT International, 2014.

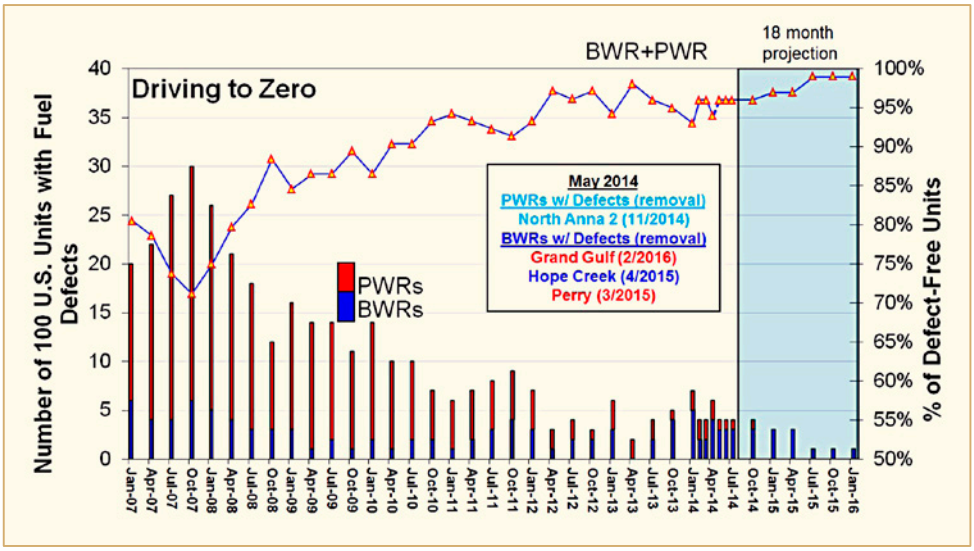

Figure 2-4: Fuel defect rates in US plants [Beale, 2014].

The source of the data presented in this Section is the Fuel Reliability Data Base (FRED) maintained by the Electric Power Research Institute (EPRI) which includes all 100 US plants (65P/35B), 24 European (9B/7P/6VVER), 45 Asian (15B/30P), 2 South African (P) and 2 South American plants (P). In terms of reactor cycles the data base includes over 700 US and about 100 non-US PWR cycles and 400 US and about 100 non-US BWR cycles [Beale, 2014]. This is the most comprehensive data base kept at this time.

The major cause of fuel failures in PWRs continues to be grid-to-rod fretting (GTRF), a cause that has been sharply reduced by improved spacer and lower nozzle designs. Once all plants have transitioned to GTRF resistant components, this failure mode is expected to be eliminated. A very low level of failures due both to debris fretting and fabrication related failures have occurred (Figure 2-5).

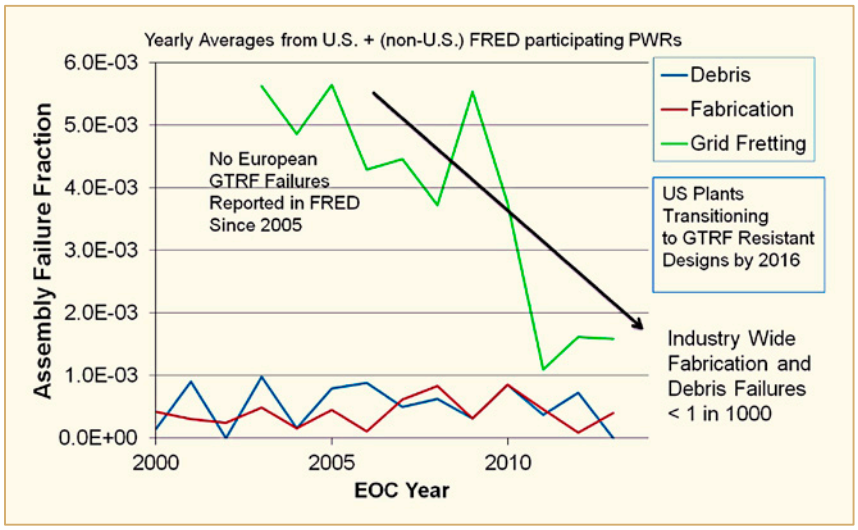

Figure 2-5: Fuel failure cause trends in FRED base PWRs [Beale, 2014].

Copyright © Advanced Nuclear Technology International Europe AB, ANT International, 2014.

The fuel failures in BWRs have been almost exclusively due to debris fretting during the past year, at a rate higher than in PWRs (Figure 2-6) An interesting comparison of debris failures in forward pumped plants with failures in full-flow demineralizer plants indicated a forward pumped plant is almost 3 times more likely to shut down with a debris failure (Figure 2-7). The forward pumped plants drain about 1/3 of the feed-water from the turbine directly into the feed-water system without going through the condenser and demineralizer in order to improve the thermal efficiency of the plant. The demineralizers are designed to remove ionic impurities in solution, however, can act as mechanical filters as well, so that they may assist in removing some debris. Erosion of the forward pumped drain piping could also add debris to the coolant. The FRED data base also shows that the probability of a debris failure is 50% higher in a cycle with a power uprate in either plant type. The debris failures tend to increase in the first cycle of the fuel and then plateau out in the second cycle [Beale, 2014].

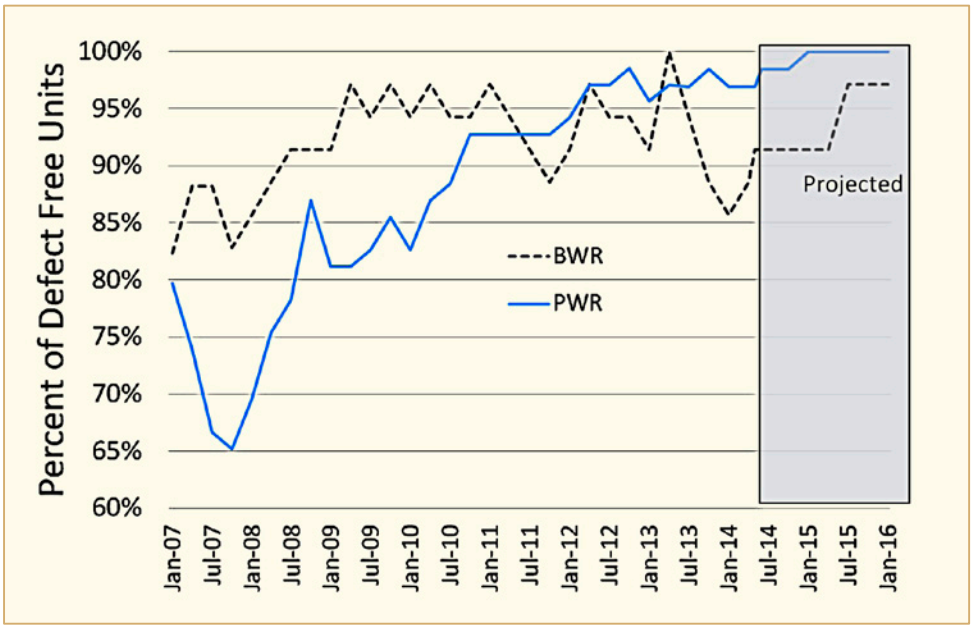

Figure 2-6: Comparison of debris failure free PWR and BWR units [Beale, 2014].

Copyright © Advanced Nuclear Technology International Europe AB, ANT International, 2014.

3 Microstructure and manufacturing (Friedrich Garzarolli)

3.1 Introduction

The microstructure is defined as the structure at the microscopic scale. The structure of a thing describes how the parts of this thing relate to each other, how they are "assembled". The microscopic scale is the one that requires a magnification device to be observed.

In metallurgy, the knowledge of the microstructure is a mandatory requirement, and has always been requested with the highest accuracy as possible. The properties of the alloys are strongly microstructure dependent.

With the same composition, the microstructure of an alloy can be deeply changed, depending of its thermo-mechanical history. Heat treatments, mechanical processing, conditions of use (a very important point in our case due to the effects of irradiation on the microstructure) induce major changes in the microstructure, inducing large changes in all the properties. Limiting our topic to engineering properties, mechanical strength, fracture toughness, corrosion resistance, creep etc. are known to depend on the microstructure.

Bridging a link between the microstructure and the properties allows the scientists to understand the mechanisms involved in the control of the property under consideration. This opens the route to improvements in the properties of the alloys and/or allows the designers to forecast changes in properties during operation (e.g. irradiation hardening or growth, changes in corrosion resistance after heat treatments.

Using the definition given above, the question to be solved with respect to the microstructure is to know what the "parts" are to be considered in the way they "relate to each other". For the microstructures of interest, three major elements have to be considered:

- The crystals are the elementary units of the metals and alloys. One has to know what is the crystallographic structure (crystallographic system, composition), what is the shape of each crystal (elongated, equiaxed), what is their relative orientation (occurrence of a crystallographic texture).

- Within the crystals, the defects have to be described accurately. Among them, we have to consider chemical defects such as clusters of foreign or solute atoms, linear defects (dislocations) and point defects (irradiation defects such as interstitials or vacancies, or chemical defects – substitutional or interstitial impurities).

- At the atomic scale, the exact chemical state and chemical environment of each atom controls its behaviour. Of interest are the oxidation state, the surrounding atoms controlling the vibration modes and therefore the mobility.

The irradiation of neutrons with energies in excess of about 40 eV will result in damage of the zirconium alloy lattice. The higher energy of the neutron and the lager the fluence, the larger lattice damage. This damage will change the zirconium alloy properties dramatically. Such changes include:

- An increase of yield and ultimate tensile strength.

- A decrease of ductility.

- An increase in corrosion rate (NB: The decomposition of the water by neutron interactions and other irradiation effects will also increase the corrosion rate by itself).

Copyright © Advanced Nuclear Technology International Europe AB, ANT International, 2014.

- An increase in rate of dimensional changes due to increases in
  - creep rate (also including residual stress relaxation).
  - irradiation growth and growth rate.

In structural materials like zirconium alloys, the overwhelming majority of defects are caused by the collision of neutrons with lattice atoms. These collisions produce vacancies and interstitials. Some of the interstitials recombine with vacancies. Others are absorbed by dislocations, which are then able to climb and concentrate between crystal planes. The remaining vacancies condense in crystal planes. Collapse of the affected lattice leads to the formation of self-interstitial and vacancy loops. They are collectively called prismatic loops and differ from loops formed by shear along a glide plane. Interstitial and vacancy loops form on prism planes and are identified by the normal to the prism plane; i.e., an <a> loop. Vacancy loops form on basal planes and are also identified by the normal to the basal plane; i.e., a <c> loop. <a> loops form relatively early in the irradiation. Their number density saturates asymptotically with increasing neutron fluence. The increase in <a> loop density increases the strength and lowers the ductility and fracture toughness of the Zr alloy material. Thus, the strength increase and ductility/ fracture toughness decrease due to this effect typically reach ~90% of their respective long-term values between 5 and 10 MWd/kgU. The ductility/fracture toughness of the Zirconium alloy may however continue to decrease with burnup due to the hydrogen pickup occurring during the corrosion reaction between the water molecule and the Zr alloy material.

The <c> type of loop induced by radiation does not form until later in life. In Recrystallized Annealed (RXA) Zircaloy-2 and -4, <c> loops are first observed at a burnup of around 15 MWd/kg and increase in density during the rest of the fuel lifetime. In Stress Relieved Annealed (SRA) Zircaloys, <c> type dislocations remain from fabrication and will result in <c> type loop formation already at start of irradiation. <c> loops are thought to strongly influence irradiation growth and creep behaviour, but probably do not affect mechanical properties. The lower irradiation growth rates of M5 and ZIRLO appear to be due to the difficulty in forming <c> loops in these alloys.

The formation of point defects such as interstitials and vacancies during irradiation will also change the creep mechanism from that during out-of-reactor conditions. The consequence is that the creep resistance ranking between different materials may be different out-of-reactor compared to in-reactor. As an example, the creep rate is larger for SRA than for RXA Zr alloy materials in-reactor while the reverse ranking is true for out-of-reactor. This means that one should be cautious in interpreting out-of-reactor creep test results for in-reactor conditions.

Corrosion resistance in zirconium alloys is intimately related to the protective part of the ZrO_2 layer (often called barrier layer) which in turn is partly related to the presence of SPPs formed in the zirconium matrix by deliberate additions of alloying elements and by heat treatments to control their size. In as-fabricated Zircaloy-4 the most common SPP is $Zr(Fe, Cr)_2$, while in Zircaloy-2 they are $Zr(Fe,Cr)_2$ and $Zr_2(Fe, Ni)$. For the ZrNb type alloys (such as M5) the most common is βNb (which is not an intermetallic). For the ZrSnNbFe alloy types (such as ZIRLO, MDA and NDA) the most common types are Zr(Nb,Fe)2 and βNb. At normal LWR temperatures (270-370°C (543-643K)) the SPPs change under irradiation in a combination of two ways – amorphization and dissolution.

Amorphization means that the original SPP crystalline structure is converted to an amorphous structure. A critical temperature exists above which the annealing processes are fast enough to prevent the accumulation of defects needed to transform crystalline SPPs to amorphous structures. For typical reactor irradiations, amorphization of both $Zr(FeCr)_2$ and $Zr_2(Fe,Ni)$ in Zry-2 occurs readily at temperatures near 100°C (373K). But, at the temperatures (300°C(573K)) and neutron flux encountered in a LWR, $Zr(Fe,Cr)_2$ becomes amorphous but $Zr_2(Fe,Ni)$ does not. Above about 330°C (603K), neither SPP becomes amorphous.

Copyright © Advanced Nuclear Technology International Europe AB, ANT International, 2014.

The fluence required to produce complete amorphization depends on neutron flux, temperature and SPP size and chemistry. But, for typical $Zr(Fe,Cr)_2$ SPPs of initial size near 0.1 μm, the entire SPP is amorphous by end of bundle life burnups, <50 MWd/KgU ($1x10^{26}$ n/m^2, E>1 MeV). The rate of dissolution depends on the SPP size, with higher rates for smaller sizes. The extent of dissolution depends on size and fluence. It has been demonstrated in a BWR that small (<0.04 βNb) SPPs in Zry-2 can completely dissolve at low to moderate burnups. Also in a PWR, but at temperature near 290°C, SPPs in Zry-4 with an average size of 0.2 μm were >80% dissolved at moderate burnup ($1x10^{26}$ n/m^2, E >1MeV). The consequence of the complete dissolution of the SPPs in Zry-2 and Zry-4 is a dramatic increase in the Hydrogen Pick-Up Fraction (HPUF) and, after some time, also an acceleration of the corrosion rate in BWRs.

For the Zr-Nb type alloys preferentially used in PWRs neither the βNb nor $Zr(Nb,Fe)_2$ SPPs become amorphous (or dissolve) for irradiation temperature >330°C (603K).

SPP amorphization in itself does not appear to affect material behaviour; however, dissolution of both amorphous and crystalline SPPs does influence corrosion and growth.

In the following subsections, more details are given on how the neutron damage changes the zirconium alloy microstructure, which in turn changes the properties of the Zr alloy material.

3.2 New results on texture and anisotropy

The paper reported in the last years on texture and anisotropy dealt mainly on fabrication, texture and anisotropy of CANDU type reactor pressure tubes and fuel rods and on the microstructural changes that may occur under a hypothetical loss-of-coolant accident.

The thesis of [Fong, 2013a], [Fong, 2013b],[Fong, 2013c] and [Fong et al, 2012] reviewed phase transformation and texture development of Zr2.5%Nb pressure tubes (PTs) and Zry-4 fuel sheet (FS) material and investigated the texture evolution, phase transformation and mechanical anisotropy using neutron diffraction during heating up to 1050°C and on cooling. The mayor topics of the study were to understand the influence of texture and the contribution of β-phase to the high-temperature anisotropic deformation behaviour of Zr-2.5Nb PT material and to determine the effect of texture on the mechanical anisotropy of Zry-4 FSs. The thesis started with a literature review of phase transformation and texture development of Zr2.5%Nb pressure tubes and Zry-4 fuel sheet material.

The fabrication of Zr2.5Nb PTs involves the following processing steps: (1st) quadruple melt ingot, (2nd) forge to bar, (3rd) machine hollow billets, (4th) preheat billets to 815°C and extrude into tubes, (5th) cold-draw 25-30% (by two wall thickness reduction steps), and (6th) stress relieve in steam-autoclave for 24 h at 400°C. The resulting microstructure consists of elongated hcp α-Zr grains containing a high dislocation density, and a thin layer of bcc β-phase at the α-grain boundaries (Figure 3-1).

The Zr-2.5Nb alloy is in equilibrium at RT in in the two-phase ($\alpha+\beta_{Nb}$) region and changes on heating to >610°C in the ($\alpha+\beta_{Zr}$) region. After extrusion at 815°C and air cooling the ($\alpha+\beta_{Zr}$) structure does not transform to the equilibrium ($\alpha+\beta_{Nb}$) structure, but remains rather as ($\alpha+\beta_{Zr}$). The final stress relief treatment at 400°C for 24 h partially decomposes the metastable β_{Zr} into a ω-phase and an enriched $\beta_{Zr.}$

At temperatures of 525°C-600°C the β_{Zr} decomposes: $\beta_{Zr} \rightarrow \alpha+\beta_{enr} \rightarrow \alpha.+ \beta_{enr}+\beta_{Nb} \rightarrow \alpha.+\beta_{Nb}$, but below 525°C: $\beta_{Zr} \rightarrow \omega+\beta_{enr} \rightarrow \alpha.+ \beta_{enr}+ \omega+ \beta_{enr} \rightarrow \alpha+\beta_{enr} \rightarrow \alpha+\beta_{enr}+ \beta_{Nb} \rightarrow \alpha.+\beta_{Nb}$. Below 525°C, however, the stable β_{Nb} phase may not be achieved, since the temperature-time-transformation (TTT) diagram for the β-phase in Zr2.5Nb pressure tubes e.g [Griffiths et al, 2008] indicates that the metastable β_{Zr} most likely transforms only into a β_{enr} phase in reasonable time periods.

As-manufactured PTs show a pronounced crystallographic texture of α-Zr grains with most of the basal poles aligned along the transverse (hoop) direction (Figure 3-2).

Copyright © Advanced Nuclear Technology International Europe AB, ANT International, 2014.

4 Mechanical properties (Kit Coleman)

4.1 Introduction

In this section we will discuss strength and ductility. Strength is expressed in terms of properties like yield strength, burst strength and hardness. Ductility is expressed in terms such as elongation at fracture or strain-to-some limit for a particular loading condition. Fracture resistance is a combination of strength and ductility that describes the conditions to initiate and grow cracks and estimate the point of crack instability. Each of these properties is affected by their alloy composition and fabrication route, and by the consequences of their residence in a nuclear reactor in hot water. Neutron irradiation changes the microstructure thereby affecting the mechanical properties. For example <a>-dislocation loops strengthen zirconium but reduce ductility and fracture toughness. Corrosion adds an oxide layer and produces hydrogen, some of which is pick-up by the components. Hydrogen is important because it forms hydrides that can lead to embrittlement. During fission, extra gasses are formed adding to the internal pressure inside a fuel rod and some elements are formed that can cause cracking, for example iodine. During service, "stresses" fluctuate so some allowance must be made for fatigue. Vibrations can produce wear and fretting that may be so severe that protective membranes are breached. All these changes have to be accommodated to assure that components function as designed. Often each of the properties is studied separately. These individual properties are then gathered into a description of the behaviour of the whole component in models and codes. Contributions to each of these items were made during the year and are summarised in the following sections.

4.2 Situations for potential damage to fuel

4.2.1 Contact

Contact between surfaces during reactor operation can produce wear and fretting. The damage can lead to wall penetration of components. The consequences may be costly: lost power generation, increased expenditures for increased chemistry monitoring of the heat-transport water, testing to identify the leaking assembly, increased contamination and risk to plant personnel, the possible need for detailed examination of the failed fuel, and complications with long term storage of the failed fuel. Thus nuclear fuel vendors and utility operators have a greater incentive to protect the fuel assemblies from contact damage. Two approaches are to minimise the unplanned contact and minimise the force of the contact. Three situations are discussed.

Copyright © Advanced Nuclear Technology International Europe AB, ANT International, 2014.

One of the most severe problems in BWRs is fretting by debris. Typically, small lengths of wire, for example from cleaning brushes, become trapped in the spacer grids. They damage the cladding when they vibrate with the water flow into contact with the fuel rod, sometimes penetrating the tube wall. [Cole et al, 2014] reported on the development of filters at AREVA. Initially the non-line-of-sight FUELGUARD™ debris filter prevented machine chips and 25 mm long pieces of wire from reaching the fuel from below the fuel stack. The next generation was designed to capture 12 mm lengths of wire, 0.3 mm in diameter, while the current version excludes wires 8 mm in length. A design of spacer strip, called ULTRAFLOW™ (Figure 4-1), encourages small segments of wire that escape the filter to bypass the grid. In tests using two-phase flow, >95% of the debris, including lengths of wire between 5 and 8 mm with diameter between 0.1 and 1 mm, safely bypassed the spacer. Although more difficult to handle than bottom-injected debris, debris from above the fuel, for example falling during refuelling, can be prevented from entering the fuel stack with a debris screen. The success of these three defences has been demonstrated with no debris failures since 2008 in the BWR at Brunswick Nuclear Plant, North Carolina. In a general review of the developments at Global Nuclear Fuel (GNF), the historical record of failure rates showed a general decline with debris damage being the current outstanding issue – note the inverse relationship with fuel cost reduction as the reliability improved, Figure 4-2 [Stachowski, 2014]. The 10x10 fuel designs have been highly reliable and resistant to well-known BWR fuel failure mechanisms. For example, no PCI-type or corrosion- or crud-related failures have occurred in over a decade because cladding material and plant water chemistry controls have greatly improved. Mitigation of debris fret failures was being addressed through both fuel design improvements, including filters, and foreign material control at plants.

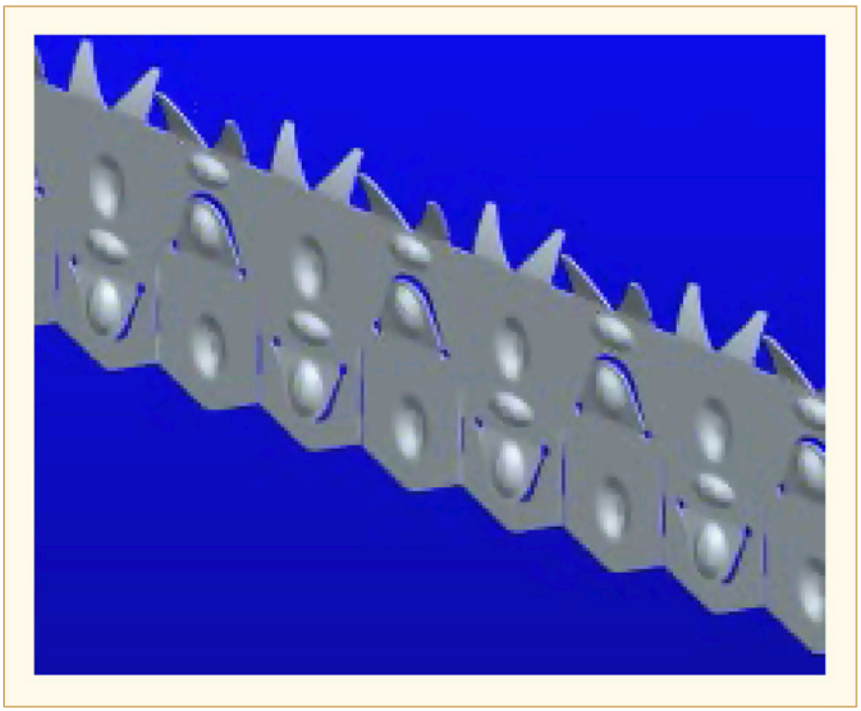

Figure 4-1: ULTRAFLOW™ spacer strip designed to prevent debris, especially wire fragments, from catching on spacer grids in a BWR [Cole et al, 2014].

Copyright © Advanced Nuclear Technology International Europe AB, ANT International, 2014.

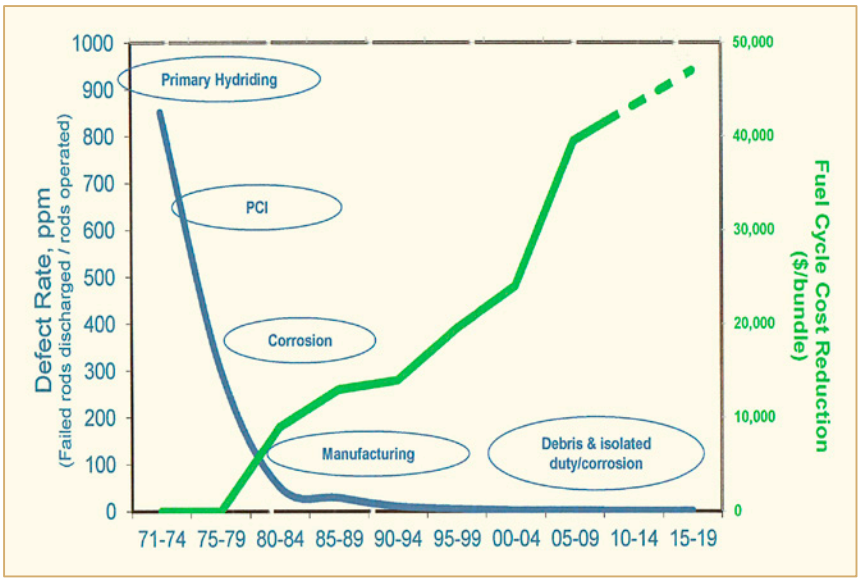

Figure 4-2: Historical record of fuel failures and reduction in fuel costs in BWRs [Stachowski, 2014].

In PWRs, wear and fretting damage to the fuel cladding at grids has caused some leakages. Testing has been done to understand the processes involved and to test possible alleviation solutions.

Laboratory experiments used a fuel rod specimen with a length that spanned three spacer grids of a typical PWR fuel assembly, about 800 mm [Lee et al, 2013]. The design of the points of contact at the springs and dimples in the grid is shown in Figure 4-3. The rod was allowed to randomly vibrate to simulate the effect of the flow of the primary coolant. The clearance between the rod and each spring and dimple was adjusted to either 0.1 or 0.25 mm (Table 4-1) to simulate relaxation by neutron irradiation and thermal degradation. The mass of the fuel was simulated with tungsten or tungsten carbide dummy pellets. Grid-to-rod fretting (GTRF) was evaluated at room temperature with water flow rates between 3 and 7 m/s and testing times up to 5 h. Random motions of the single rod specimen were measured by two non-contacting displacement transducers. The amplitudes of the vibrations of the six configurations are depicted in Figure 4-4. The amplitude increased with increase in the number of large clearances and yielded irregular peaks in AS3 and AS6. The volume of wear damage is included in Table 4-1. Although the results of wear experiments are notoriously irreproducible, the values were inversely related to the maximum amplitude of rod vibration (Figure 4-5). This result suggests that wear damage from impacting is smaller than abrasive rubbing, in agreement with previous results [Ko, 1979].

Copyright © Advanced Nuclear Technology International Europe AB, ANT International, 2014.

5 Dimensional stability – Charged particle bombardment of Zr alloys (Ron Adamson)

These results are presented in ZIRAT19/IZNA14 Special Topic Report "Charged Particle Bombardment of Zirconium alloys".

Copyright © Advanced Nuclear Technology International Europe AB, ANT International, 2014.

6 Corrosion and hydriding (Friedrich Garzarolli)

6.1 Overview on nodular corrosion

6.1.1 Introduction

Nodular corrosion on Zry-2/4 or E110 fuel rods and structural components can arise in BWRs or RBMKs. Nodular corrosion appears in on Zry-2/4 or E110 under the typical operation temperature only under irradiation and only in an oxidative environment.

The nodular oxide is a locally much thicker oxide that forms within the relatively thin uniform oxide. Visually it appears as white spots in the else thin black uniform oxide and metallographic as locally thicker oxide with different forms (lenses, mushrooms, etc.) as shown in Figure 6-1. It can vary significantly between different BWRs, cycles, and material lots (Figure 6-2). It is well known that *the tendency for nodular corrosion of Zry-2/4 increases with increasing process temperatures and times*, affecting SPP size and solute content.

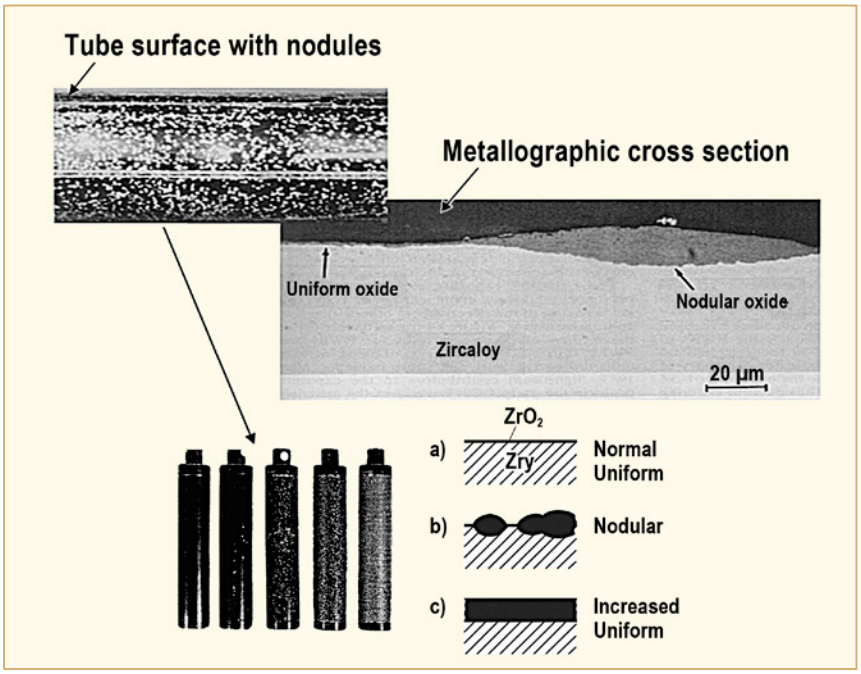

Figure 6-1: Typical appearance of nodular corrosion in visual inspection and metallographic examination [Adamson et al, 2007/2008].

Copyright © Advanced Nuclear Technology International Europe AB, ANT International, 2014.

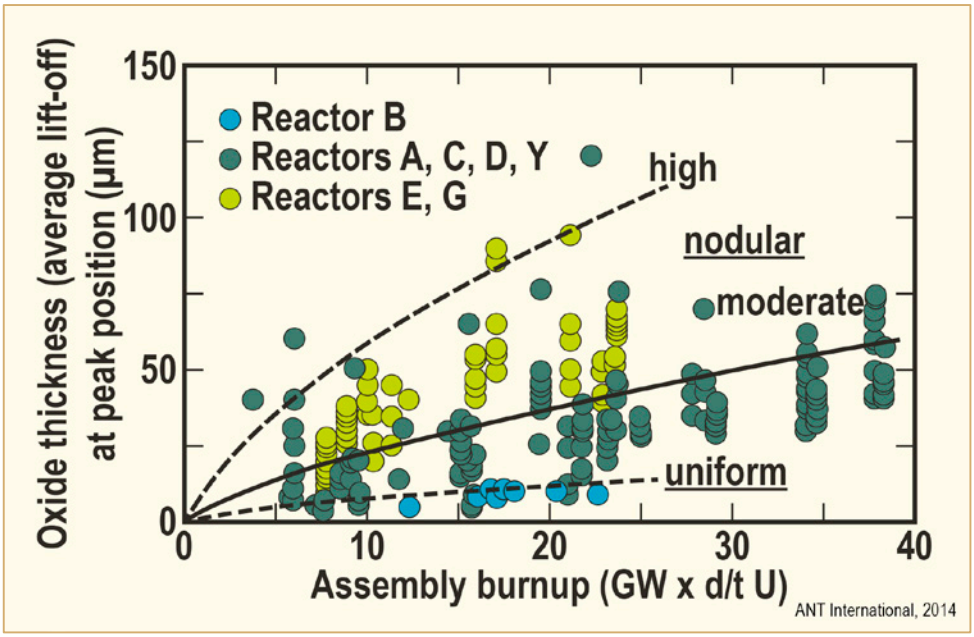

Figure 6-2: Uniform (lower curve) and nodular corrosion (two upper curves) of BWR Zry-2 fuel rods irradiated during 1965-1980, after [Garzarolli & Stehle, 1986].

Nodule nucleation occurs in BWR usually after 10 to 20 days for Zry-2 and after 30-100 days for Zry-4 [Garzarolli & Sell, 2006]. The nodular corrosion is characterized by the formation of irregularly shaped patches of thick oxide, which grows laterally on the surface but also in depth with increasing BU or fluence. The nodules can in extreme cases grow together, coalesce, on the material surface and form a thick uniform nodular oxide.

The tendency for nodular corrosion depends largely on the particular reactor water chemistry and on the microstructure of the Zircaloy material, especially the size and distribution of the second phase particles (SPPs) and possibly the Fe, Cr, and the Ni solute content, which depends on fabrication temperatures and times as well as ingot chemistry.

Only Sn-free Zr alloys may form nodular corrosion out reactor in 300°C water after long exposure times (>1000 d) [Garzarolli et al, 1994]. Otherwise nodular corrosion can only be formed out of reactor on sensitive Zry-2/4 lots at temperatures >450°C, and exposure times of ≤24 h at >490°C, as can be seen from Figure 6-3.

Copyright © Advanced Nuclear Technology International Europe AB, ANT International, 2014.

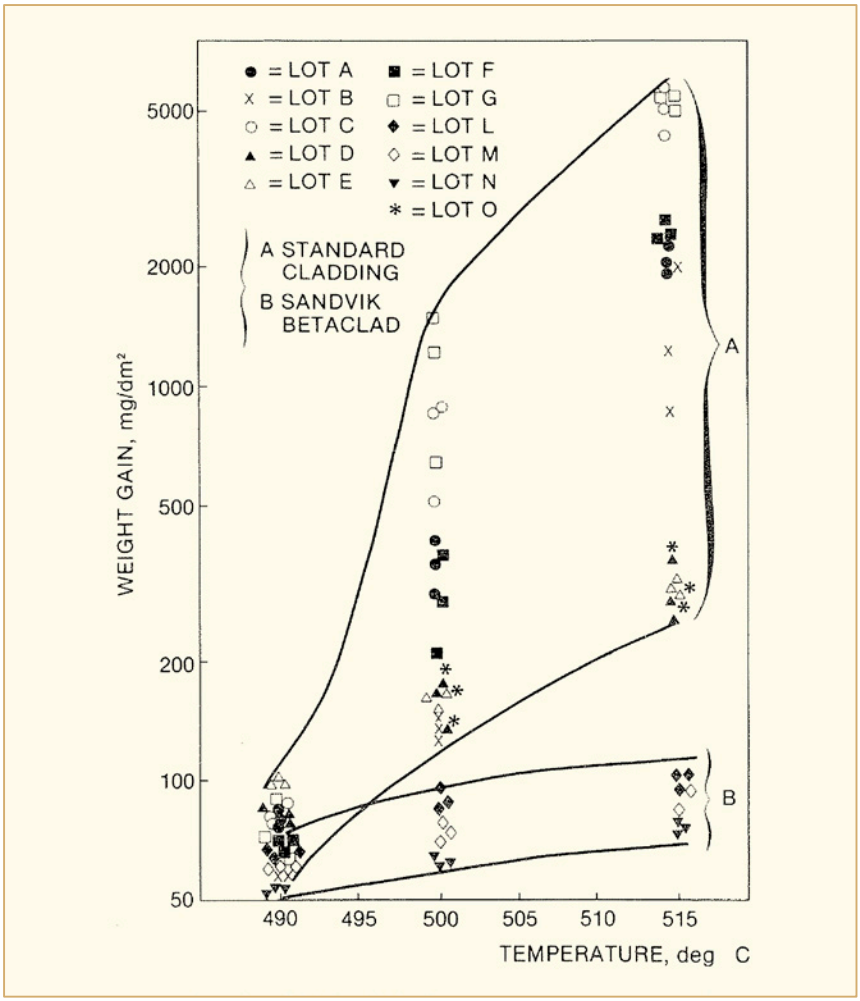

Figure 6-3: Effect of test temperature on weight gain in autoclave testing in steam at 125 bar for 24h [Andersson & Thorvaldsson, 1987].

6.1.2 Growth of nodular oxide

Nodular corrosion oxide thickness correlates to burnup (Figure 6-4). Often the peak oxide thickness is seen in the lower part of the fuel rod, where boiling starts and where CRUD deposition becomes significant.

Copyright © Advanced Nuclear Technology International Europe AB, ANT International, 2014.

7 Primary failure and secondary degradation – open literature data (Peter Rudling)

The open literature data are provided in the following sections.

7.1 Introduction

7.1.1 Primary failures

During reactor operation, the FR may fail due to a primary cause such as fretting, PCI manufacturing defects, corrosion, etc. (Table 7-1).

Table 7-1: Primary failure causes for LWR fuel during normal operation and Anticipated Operational Occurrences (AOO).

Primary failure cause	Short description
Excessive corrosion	An accelerated corrosion process results in cladding perforation. This corrosion acceleration can be generated by e.g., CRUD deposition (CILC)[a], Enhanced Spacer Shadow Corrosion, (ESSC)[b], (in BWRs), dry-out due to excessive FR bowing.
Localised hydriding	Fuel may fail in hydrided regions fractured under tensile loading that arose with accumulation of exposure during the course of normal operation (BWRs)[c]. Li seems to be involved in the failure mechanism (It is not clear from where the Li originated since Li does not normally occur in BWR coolants). More work is needed to understand the mechanism that led to the localised hydriding.
Manufacturing defects	Non-through-wall cracks in the fuel cladding developed during the cladding manufacturing process. Defects in bottom and/or top end plug welds. Primary hydriding due to moisture in fuel pellets and or contamination of clad inner surface by moister or organics. Too large a gap between the FR and the spacer grid supports (poor spacer grid manufacturing process) leading to excessive vibrations in PWR fuel causing fretting failures. Chipped pellets may result in PCI failures both in liner and non-liner fuel.
PCI	PCI—an iodine assisted SCC phenomenon that may result in fuel failures during rapid power increases in a FR. There are three components that must occur simultaneously to induce PCI and they are: 1) tensile stresses—induced by the power ramp, 2) access to freshly released iodine-occurs during the power ramp, provided that the fuel pellet temperature becomes large enough and 3) a sensitised material—Zircaloy is normally sensitive enough for iodine stress-corrosion cracking even in an unirradiated state.
Cladding collapse	This failure mechanism occurred due to pellet densification. This failure mode has today been eliminated by fuel design changes and improved manufacturing control.
Fretting	This failure mode has occurred due to: Debris fretting in BWR and PWR. Grid-rod fretting – Excessive vibrations in the PWR FR causing fuel failures. This situation may occur for example due to different pressure drops in adjacent FAs causing cross-flow. Baffle jetting failures in PWRs – Related to unexpectedly high coolant cross-flows close to baffle joints.
[a]CILC – an accelerated form of corrosion that has historically resulted in a large number of failures in BWRs. Three parameters are involved in this corrosion phenomenon, namely: 1) Large Cu coolant concentrations as a result of e.g., aluminium brass condenser tubes, 2) Low initial fuel rod surface heat flux – occurs in Gd rods and 3) Fuel cladding that shows large initial corrosion rates- occurs in cladding with low resistance towards nodular corrosion. [b]This corrosion phenomenon resulted in a few failed rods. The mechanism is not clear but seems to be related to galvanic corrosion. This corrosion type may occur on the fuel cladding in contact or adjacent to a dissimilar material such as Inconel. Thus, this accelerated type of corrosion occurred on the fuel cladding material at spacer locations (the spacer springs in alloy BWR fuel vendors fuel are made of Inconel). Water chemistry seems also to play a role if the fuel cladding material microstructure is such that the corrosion performance is poor. Specifically coolant chemistry with low Fe/(Ni±Zn) ratio seems to be aggressive (provided that the cladding material shows poor corrosion performance. A fuel cladding material with good corrosion resistance does not result in ESSC, even in aggressive water chemistry. [c]Sixty-three GE13B 9X9 fuel assemblies in Browns Ferry, Unit 2 (BF2) during Cycle 12 failed. Seven rods were examined in hot cell to determine the primary failures cause.	
ANT International, 2014	

Copyright © Advanced Nuclear Technology International Europe AB, ANT International, 2014.

Table 7-2 and Table 7-4 provide key data for some of the most recent fuel-failure cases.

Table 7-2: Summary of previous PWR/PHWR failure key events, see previous ZIRAT/IZNA-reports for details. New results added to the table from the ZIRAT18/IZNA13 report is in red text.

Nuclear unit	Type of primary failure	Comment
TMI-1, Cy 10, 1995	Nine high peaking FRs, Zry-4 Cladding, failed after 122 days of operation. CRUD/corrosion related failures.	All failed and degraded pins reportedly had Distinctive CRUD Pattern (DCP)[3]. High peaking factors, thermal-hydraulic conditions. Calculations indicated that no boiling should have occurred on the pins with DCP, although the pins with DCP were calculated to have a slightly higher temperature. Water chemistry (low pH at BOC, pH < 6.9, max LiOH 2.2 ppm). Some, AOA effect was found reaching a maximum in the middle of cycle 10. The source of the CRUD could not be determined. The CRUD sampling showed that the nickel-to iron ratio was in the range 1.25 to 16.7, which was reportedly somewhat lower than in previous investigations.
Seabrook, Cy 5, 1997	Five one-cycle ZIRLO rods failed. CRUD/corrosion related failures.	Longer cycle in transition to 24-month cycle. Possibly CRUD-induced overheating resulting in substantial nucleate boiling.
EdF data reported in 2009 [Thibault et al, 2009]	The main failure causes in the EdF plants are: GTRF wear, Clad manufacturing defects and, Excessive fuel assembly bowing (resulting in assemblies grids hanging-up during loading and unloading and IRI)	A significant number of fuel failures were related to the M5 fuel cladding in 1300 MWe and 1450 MWe units. The M5 FR failures were due to fabrication defects either related to the end plug girth or fill hole weld or defects in the fuel clad itself at grid levels (related to the pulling of the rods into the assembly structure). To resolve these manufacturing issues, AREVA has modified the welding techniques as well as the rod pulling procedure. It was observed that there were no GTRF failures in 2008 (in previous years there have always been some GTRF failures). The reasons for the great improvement is thought to be due to that both AREVA and Westinghouse have introduction reinforced FAs design (AFA3GLr – AREVA and RFA2- Westinghouse). Since the introduction of the AREVA AFA3G design in 1999, a decrease of the average core bow in EdF NPPs has been observed, especially on the 900 MW units, but not as fast as expected. The maximum values of bowing remain relatively high on the 1300 MW units, typically between 15 and 19 mm for a “S shape” bow. The Westinghouse RFA fuel design behaves in the same way with similar bowing range while HTP assembly deformations are twice less. Incomplete Rod Insertions (IRIs) due to bowing have been significantly reduced since the AFA3G FA’s design has been loaded in EdF NPPs and despite the increasing of the average discharge burnup of the FAs. In 2008, no anomaly of RCCA drop time was observed in EdF NPPs during the BOC tests. Concerning the EOC tests, no anomaly was observed in the 12 feet units whereas four RCCAs dropped without recoil in the 14 feet units. Three of them was AFA3G FAs (two “2nd cycle” FAs and one “4th cycle” FA) and one was the older design (AFA2G). The number of FAs damaged during handling operations has decreased in 2008 but remains significant. The damages concern only AFA 2G or 3G design and mainly the 14 feet units. It occurs during the unloading operations. The damages generally occur during a “three-sided box” extraction and result from grids’ hanging due to bowing and to a reduced gap between FAs following unexpected grid growth due to re-crystallized Zircaloy-4.

[3] This acronym implies that the fuel inspection revealed CRUD deposits on the fuel rod and that the deposits were uneven in the rod circumference.

Copyright © Advanced Nuclear Technology International Europe AB, ANT International, 2014.

Table 7-3: (cont'd) Summary of previous PWR/PHWR failure key events, see previous ZIRAT/IZNA-reports for details. New results added to the table from the ZIRAT18/IZNA13 report is in red text.

Nuclear unit	Type of primary failure	Comment
Kakrapara Atomic Power Station (KAPS) unit#2, India	Manufacturing defect	A PHWR fuel rod with an incomplete fusion end plug weld. The fuel rod operated at very low power for the first 18 months as the fuel bundle was in a peripheral location of the core during that period. For the next 5 months, the fuel pin operated at a linear power rating of 410 W/cm when the fuel bundle was shifted to a high flux location in the core. In total the rod operated in failed condition for a period of 710 days and accumulated a burnup of 4400 MWd/tU. See ZIRAT18/IZNA13 AR for more details.
Korean PWR plant, identification not known	2 debris-induced fuel failures	PWR debris-induced fuel failures on a thrice-burned fuel rod, not showing any degradation and a first-burned fuel rod, which degraded. See ZIRAT18/IZNA13 AR for more details.
		ANT International, 2012

Table 7-4: Summary of previous BWR failure key events, see previous ZIRAT/IZNA-reports for details. New results added to the table from the ZIRAT18/IZNA13 report is in red text.

Nuclear unit	Type of primary failure	Comment
KKL	1997, 1998	Excessive Shadow Corrosion on LK II Zry-2 Cladding under the Inconel x-750 grid springs. The oxide thickness was locally above 500 µm. The most notable cladding corrosion attacks were found on fuel that had experienced a fourth, fifth, or sixth operational cycle. Zn-injection. Low level of Fe in coolant.
River Bend	Cy 8, 1999	At least 12 GE First cycle FRs were failed. Heavy CRUD – The failures appeared in bundles with a significant iron CRUD deposition. The heavy deposits almost filled the gaps between the FRs. Some 700 pounds (320 kg) iron was estimated to have been input to the River Bend-1 RPV during cycle 8 (1998-1999). CRUD deposit thickness in the range 37–55 mils (940 – 1400 µm) was reported. Analysis of the CRUD showed that the major phases were hematite and spinel, reportedly magnetite or zinc ferrite. Significant amounts of copper, up to 15% were found in some cases. No NMCA. Zn-injection.
Vermont Yankee, 2001-2002	5 FRs failed due to CRUD corrosion.	A total of 5 failed GE rods in 4 bundles were removed from the core at Vermont Yankee in a mid-cycle outage in May 2002, along with 40 other bundles deemed most at risk of failure due to being similar to the leakers in terms of duty, exposure, and tubing material.
Browns Ferry 2, Cy 12, 2001-2003	63 FAs failed due to localised massive hydriding	Affected fuel was GE13B claddings that failed in their second cycle with burnups of 29-30 MWd/kgU. Bundles that failed tended to be leading for the reload batch, indicating some impact of duty on tendency for failures. HWC started in BOC Cy 11 and NMCA at EOC 11 was implemented (3/01), Depleted Zinc Oxide (DZO) started in 1997 at 3 to 5 ppb. Maximum oxide thickness both in lower and upper part of the failed rods. Maximum CRUD deposition towards the bottom of the rods. BF2 changed out their condenser tubes to Ti-tubes 8-10 years ago. Cladding material - Corrosion behaviour was sensitive to alloying content, primarily iron and tin; - Multiple ingots were affected; - Ingots supplied by two different vendors were affected. An update of the root cause examinations of the sixty-three failed GE13B 9X9 fuel assemblies in Browns Ferry, Unit 2 (BF2) during Cycle 12 was presented. Seven rods were examined in hot cell to determine the primary failures cause. The authors, [Lutz et al, 2012] and [Lutz et al, 2013] suggest that the BF2 Reload 10 fuel failed by hydrided regions fractured under tensile loading that arose with accumulation of exposure during the course of normal operation. The results also suggest that Li contributed to the failures at least by aggravating the late stage corrosion of the BF2 Reload 10 rods, regardless of any role it may have had in initiating the corrosion. See ZIRAT18/IZNA13 AR for more details.

Copyright © Advanced Nuclear Technology International Europe AB, ANT International, 2014.

8 Cladding performance under accident conditions LOCA and RIA (Peter Rudling)

8.1 Introduction

8.1.1 Loss of Coolant Accident

The design basis Loss of Coolant Accident (LOCA) is a break in a pipe that provides cooling water to the reactor vessel. Analyses are performed for a variety of break sizes and locations to demonstrate that the ECCS can maintain the fuel in a coolable geometry. The limiting break is typically in one of the cold, main coolant pipes of a PWR or one of the intake pipes to the recirculation pump of a BWR.

The LOCA process starts by the decrease and ultimate loss of coolant flow at the same time that the reactor is depressurized (Figure 8-1). The loss of coolant flow decreases heat removal from the fuel, increasing the fuel temperature and causing a significant temperature rise of the cladding. The decrease in system pressure causes an outward pressure differential and a hoop stress in the cladding wall. The result is the plastic deformation, or *ballooning* of the cladding. Ballooning may also result in *fuel relocation*[12] that may impact the cladding temperature as well as the Equivalent Cladding Reacted (ECR[13]) in the later phase of LOCA.

Ballooning of the fuel rods may result in *blockage* of the coolant sub-channel that in turn may impact the fuel coolability. If large fuel clad burst strains occur at the same axial elevation, *co-planar deformation*, in the FA, the coolability may be significantly degraded. Specifically, the clad azimuthal temperature gradient will strongly impact the burst strain. The extent of the ballooning is also dependent on:

- Creep strength of the cladding.
- Stress in the cladding and the corresponding strain rate.
- Temperature and the rate of temperature increase.

Depending on the temperature, the cladding ductility and the rod internal pressure, the cladding will either stay intact or may burst which will allow steam to oxidize the fuel clad inner surface. In addition, some of the hydrogen released by the water/zirconium corrosion reaction inside the burst fuel may be picked up by the cladding resulting in very high local hydrogen concentrations (1000-3000 wtppm H). A fuel cladding with such high hydrogen concentrations will be very brittle even though the cladding is not oxidised at all, i.e. ECR is 0. The fuel clad axial temperature distribution will determine the axial elevation of the ballooned and burst fuel rods in the assembly. The axial and azimuthal fuel clad temperature distribution is a result of the heat transfer mechanisms at the surfaces of the cladding.

[12] Fuel relocation may occur, if during LOCA a section of the fuel rod experiences ballooning, by slumping of fuel fragments from upper location in the ballooned section.
[13] The ECR is defined as the total thickness of cladding that would be converted to stoichiometric ZrO_2 from all the oxygen that are contained in the fuel cladding as ZrO_2, and oxygen in solid solution in the remaining clad metal phase.

Copyright © Advanced Nuclear Technology International Europe AB, ANT International, 2014.

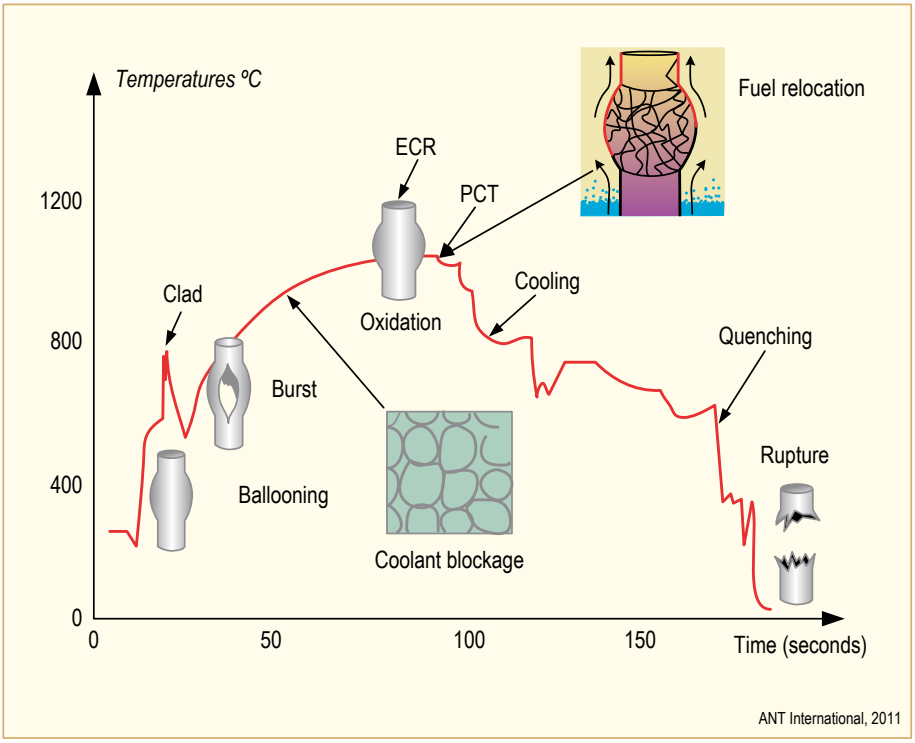

Figure 8-1: Typical LOCA in a PWR.

The increasing temperatures and presence of steam will cause the intact cladding to oxidize on the OD and the burst cladding to oxidize on both the OD and ID (two sided oxidation) until the ECCS is activated and the water quenches the cladding. The oxidation process at the high LOCA temperatures will increase the oxygen and hydrogen content in the cladding, reducing its ductility and resistance to rupture. The process and final structure of the cladding after a LOCA cycle is shown in Figure 8-2.

Copyright © Advanced Nuclear Technology International Europe AB, ANT International, 2014.

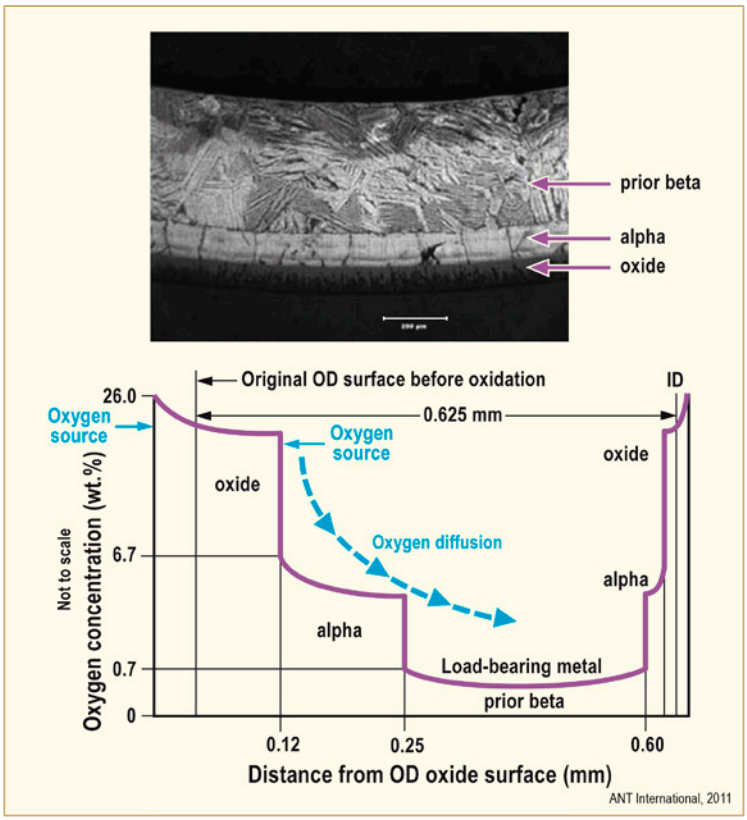

Figure 8-2: Structure of oxidized cladding, after [Meyer, 2013].

- First, the high water and steam temperatures increase their reaction rates with the cladding and increase the conversion of the cladding surface into thicker ZrO_2 films.
- As the LOCA temperature passes the levels where α→β transformations start and finish, the resulting structure consists of:
  - The growing ZrO_2 layer.
  - A brittle zirconium alloy layer with a very high oxygen content which stabilizes the α phase, formed by diffusion of oxygen from the oxide layer.
  - The bulk cladding, which is now in the β phase, has a high solubility for hydrogen; the hydrogen picked up by the cladding from the water-metal reaction increases the solubility of oxygen in the β layer.
- The ZrO_2 and oxygen stabilized α layers grow with continued diffusion of oxygen and hydrogen from the water reaction. The increasing amount of oxygen convert some of the β phase to oxygen stabilized α phase with the concurrent shrinkage of the β phase. The remaining β phase cladding wall thickness is transformed to α phase, or "prior β phase", on cooling and is the only structural part of the cladding that can insure its integrity.

Copyright © Advanced Nuclear Technology International Europe AB, ANT International, 2014.

9 Dry Storage (Charles Patterson)

9.1 Introduction

Managed, recoverable storage of irradiated fuel continues to be an essential aspect of water-reactor fuel cycles throughout the nuclear community. As of the latest comprehensive survey (mid-2010), about 225 000 tons of used or spent nuclear fuel (SNF)[15] is being stored around world [Sokolov, 2010]. The inventory of SNF is increasing by about 6800 tons per year and is expected to reach ~445000 tons by 2020, [IAEA, 2008]. Estimates of SNF inventories at the end of 2010 are shown by country in Table 9-1.

Table 9-1: Estimated SNF inventories at the end of 2010 by country, after [Peachy, 2012].

Country	SNF Inventory (MTM)		Notes
	Current	Projected	
Belgium	---	5 000	
Canada	42 946	92 000	
Finland	1 820	5 500	
France	13 772		Active reprocessing program
Germany	6 801	10 800	Projected does not reflect current phase-out policy
Hungary	980	2 123	
Japan	16 714		March 2011; reprocessing program being developed
Korea	10 761	71 000	December 2009
Russia	19 240		Active reprocessing program
Sweden	5 818	12 000	
Switzerland	1 240	3 575	
UK	5 850		December 2007; reprocessing program
USA	65 000	130 000	
Ukraine	4 651		July 2008
ANT International, 2014			

Spent fuel is being stored in pools that are either located in reactor buildings or are located away from reactors and in dry containers located at reactor sites or at separate storage facilities. Worldwide, over 80% of SNF is stored in pools [IAEA, 2012b], with increasing amounts in dry storage systems. The methods of storage are summarized by country in Table 9-2.

[15] The term "Spent Nuclear Fuel" is used collectively in this report to refer to nuclear fuel that is described in literature and regulations as either "used" or "spent". In this case, SNF refers to irradiated fuel that will be stored in a recoverable manner prior to reprocessing or permanent disposal regardless of its initial, post-discharge disposition.

Copyright © Advanced Nuclear Technology International Europe AB, ANT International, 2014.

Table 9-2: Spent fuel storage methods by country, after [Peachy, 2012].

Country	On-site storage			Centralized storage		
	AR Wet	AFR Wet	Dry	Wet reprocessing	Wet aging	Dry
Argentina	X		X			
Armenia	X		X			
Belgium	X	X	X			
Brazil	X					
Bulgaria	X		X			
Canada	X		X			
China	X		X	X		
Czech Republic	X		X			
Finland	X	X(UC)				
France	X			X		
Germany	X		X			X
Hungary	X					X
India	X			X		X
Italy	X				X	
Japan	X	X	X	X		X(UC)
Korea	X		X			
Mexico	X					
Netherlands	X					
Pakistan	X					
Romania	X		X			
Russia	X			X	X	X
Slovakia	X	X				
Slovenia	X					
South Africa	X		X			
Spain	X		X			
Sweden	X				X	
Switzerland	X	X	X			X
Taiwan	X		X(UC)			
UK	X		X	X		
Ukraine	X		X			
USA	X		X			

Notes:
AR = At reactor
AFR = Away from reactor
UC = Under construction

ANT International, 2014

Copyright © Advanced Nuclear Technology International Europe AB, ANT International, 2014.

10 Dysprosium Hafnate – A new absorber (Alfred Strasser)

10.1 Introduction

The currently used absorbers in LWRs, the 80% silver (Ag) – 15% indium (In) – 5% cadmium (Cd) alloy and boron carbide (B_4C), are both subject to swelling that can result in the cracking of the cladding and put an end to its mechanical life before its nuclear life limit is reached. The irradiation induced transmutation of ^{10}B to helium (He) and lithium (Li) in B_4C and the transmutation of In to Sn in the AgInCd alloy result in a volume increase that interacts with the cladding and produces strains that crack the cladding. Additional disadvantages of these absorbers are the poor corrosion resistance of the B_4C cladding in case of cladding rupture and the relatively low melting point of the AgInCd alloy.

The Russian VVER 1000 PWR plants also used B_4C for the absorber in their control rods and were faced with the same swelling induced cracking problems as the Western BWRs and some PWRs. Their control assemblies (CAs) are similar to the Western concept of a set of absorber rods attached to a spider and entering the fuel assembly guide tubes during their power control function. The VVER-1000 has 61 CAs of which 10 are used as power control rods and 51 as shutdown rods. Each CA has 18 rodlets with absorbers clad in stainless steel.

The original design had vibratory compacted (vipac) B_4C at 1.7 g/cm^3 (67% of theoretical density) for the entire length of the rodlet. The cladding was 18% Cr, 10% Ni, Ti stabilized stainless steel (X18H10T), 8.2 mm diameter with a 0.6 mm wall thickness containing an absorber length of 3700 mm. The operation of these assemblies was satisfactory until experience in the Novovoronezh Plant indicated that in 3 years of power control rod operation or 7 years of shutdown rod operation the cladding diameter increased 0.7% and 2% respectively and initiated cracking. The length of this exposure corresponded to about 45-50% ^{10}B depletion, similar to that experienced by the Western BWRs. This initiated their search for an improved absorber and resulted in the development of dysprosium (Dy) ceramics for application to their VVER 1000 reactors [Zakharov et al, 2011].

A number of design changes were evaluated by test reactor irradiations and these included the substitution of hafnium (Hf) metal or dysprosium titanate (Dy_2O_3 . TiO_2), (abbreviated as "DyTi" in this report) for the B_4C in the tip of the rodlets and the substitution of a nickel base alloy with 42% Cr and 1% Mo (EP630U) or Hf tubing for the stainless steel cladding. The choice of Hf was based on its good nuclear and mechanical properties, good corrosion resistance and dimensional stability during irradiation, with the downside of potential hydriding and irradiation growth. The irradiated alloy EPU630U, as well as the Hf, indicated an unusual retention of ductility, with a potential for surviving the B_4C swelling related stresses [Ponomarenko et al, 2000].

The Dy absorber was chosen on the basis of its stable transformation products, primarily other Dy isotopes, as noted in Section 2. This was initially confirmed by the irradiation and examination of DyTi powder after 4 years of exposure as a power regulating rod in Novovoronezh, that showed no rodlet dimensional changes, no swelling or sintering of the vipac DyTi powder and no outgassing during irradiation. This was countermanded by subsequent tests that reported the compound as "unstable" due to a second phase initiated swelling that could be formed during fabrication and proposing a more stable compound of Dy_2O_3. HfO_2 ("DyHf" in this report) [Risovany et al, 2006]. The overall development of the absorber materials is shown in Figure 10-1.

Copyright © Advanced Nuclear Technology International Europe AB, ANT International, 2014.

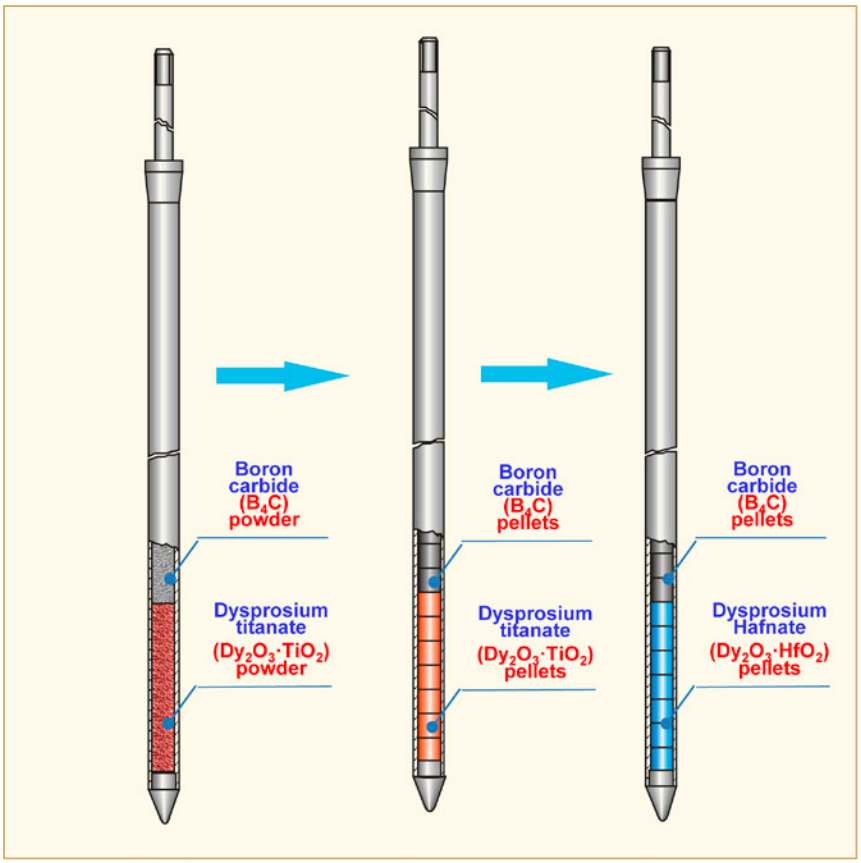

Figure 10-1: Development of control rods for VVER-1000 plants [Zakharov et al, 2014].

The currently available data on the transmutations, properties, fabrication and performance of DyHf are the topics of this Section.

10.2 Transmutations and nuclear properties

The choice of Dy was based on its transmutation into other high cross-section Dy isotopes and the lack of gaseous transmutation products that could promote high swelling rates. The decay products include holmium (Ho) and erbium (Er), (Figure 10-2). The Dy isotopic composition is shown as a function of rodlet length after 4 years of exposure in the Novovoronezh Unit 5 on Figure 10-3. The change in composition from the bottom toward the top of the rod is representative of the decrease in fluence exposure.

Copyright © Advanced Nuclear Technology International Europe AB, ANT International, 2014.

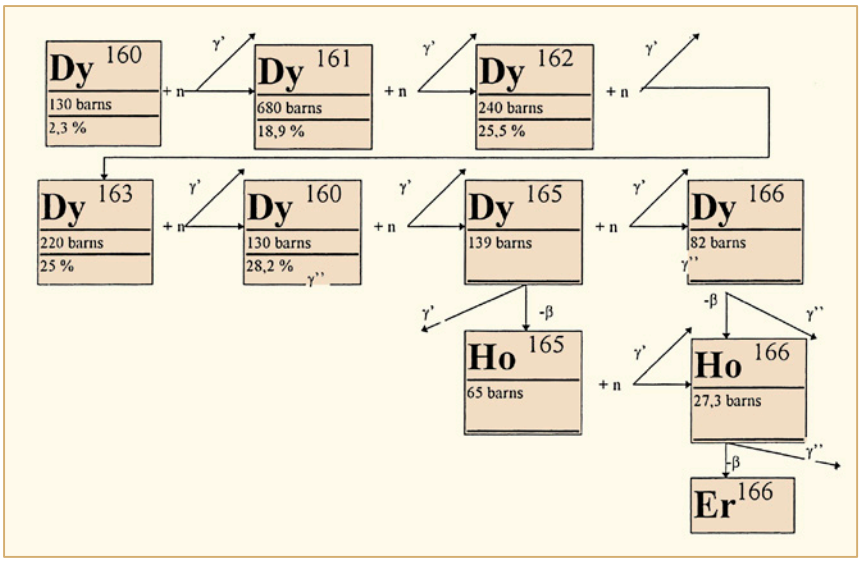

Figure 10-2: Transformation chain of dysprosium in the energy interval from 1 to 100 eV (corrected version [Chernishov & Troyanov, 1997]).

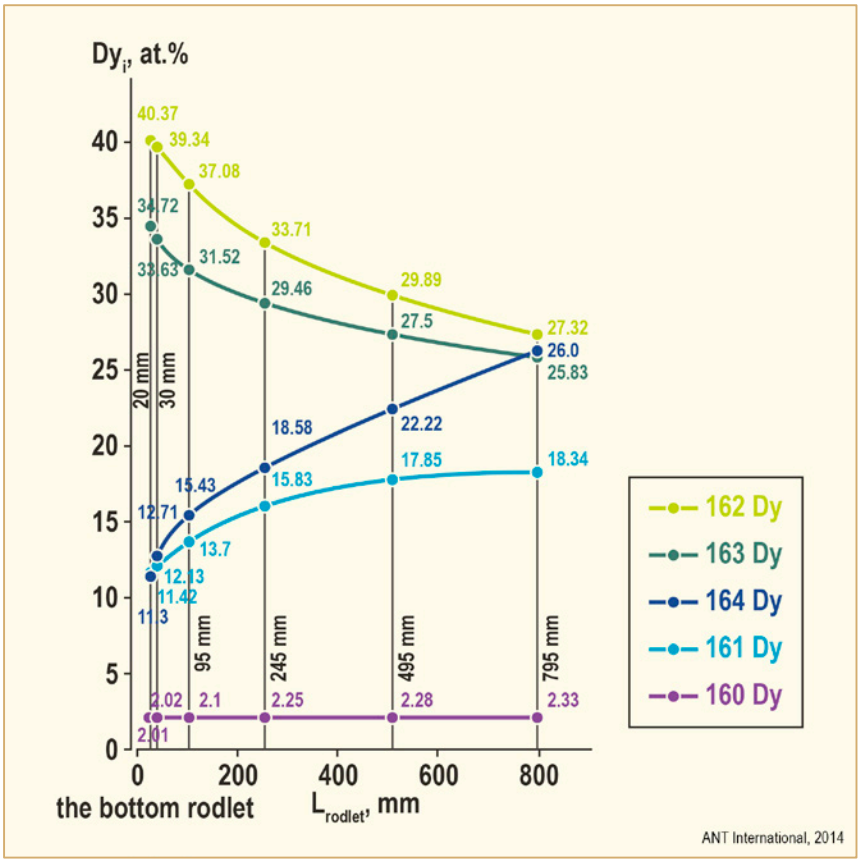

Figure 10-3: Change of Dy isotopic composition along a rodlet after irradiation for 4 years in a VVER1000, after [Ponomarenko et al, 2000].

Copyright © Advanced Nuclear Technology International Europe AB, ANT International, 2014.

11 Trends and needs

Improved fuel reliability and operating economics are the driving forces for changing operating conditions, while at the same time maintaining acceptable margins to operating and regulatory safety limits. Table 11-1 gives the trends for BU achieved compared to regulatory limits in various countries. An approximate ("rule of thumb") conversion of BU to fluence is 50 GWd/MT is equivalent to about $1x10^{22}$ n/cm^2, E>1 MeV (or about 17 dpa), but this depends on many nuclear parameters such as enrichment, extent of moderation and neutron energy spectrum. In general PWRs operate to higher discharge BUs compared to BWR because of higher PWR power densities and neutron fluxes, but the differences are decreasing with time. There are some incentives to reach BUs of 60-70 GWd/MT batch average, but the economic values of doing so are decreasing. A majority of US plants and many in Europe have undergone power uprates, from a few percent to up to 20%. This increases the number of FAs in a core that operates at high power, thereby decreasing the margin to established limits. In cooperation with utilities, fuel suppliers have operated LTA or LUAs to very HB, in some cases approaching 100 GWd/MT peak rod exposures.

Table 11-1: Maximum BUs achieved vs. regulatory limits, (excludes LTAs).

	BU (GWD/MT)				
Country	**Batch**	**Assembly**	**Rod**	**Pellet**	**Regulatory Limit**
USA	57	58	62	73	62.5 peak rod
Belgium		50-55			55 UO_2 assy., 50 MOX assy.
Czech Republic	51	56	61		60 peak rod
Finland	45.6*	48.6	58		57 assy. (for PWR)
France	47	51 UO_2 42 MOX			52 assy.
Germany	58	62	68		65 assy.
Hungary		50	62		
Japan	50	55	62		55 UO_2 assy., 45 MOX assy.
Korean Republic	46				60 rod
Netherlands	52	55	59		60 rod
Russia	60	65			
Spain	50.4	57.4	61.7	69	
Sweden	47	57.2	63.6	65	60 assy., 64 rod
Switzerland	64	68	73		80 pellet
Taiwan					60 rod (P), 54 assy. (B)
UK	44.3	46.5	50		55 pellet
Ukraine		50			
*Current batch design for 50 GWD/MT in BWR					
					ANT International, 2014

Copyright © Advanced Nuclear Technology International Europe AB, ANT International, 2014.

12 References

10 CFR Part 100.11, *Determination of Exclusion Area, Low Population Zone, and Population Centre Distance*, U.S. Government Printing Office, Washington, 1990a.

10 CFR Part 50 Appendix A, *General Design Criteria for Nuclear Power Plant*s, U.S., Government Printing Office, Washington, 1990b.

Abe H., Abe T. , Kishita S. , Kano S., Satoh Y. and Matsukawa Y., *Development of an Advanced Method for Expansion Due to Compression, Testing*, Proceedings of WRFPM 2014, Paper No. 100165, Sendai, Japan, Sep. 14-17, 2014.

Adamson R. B., Lutz D. R. and Davies J. H., *Hot Cell Observations of Shadow Corrosion Phenomena*, Proceedings Fachtagung der KTG-Fachgruppe, Brennelemente und Kernbautelle", 29 Februar/1 Marz 2000, Forschungszentrum Karlsruhe, 2000.

Adamson R. B., Cox B., Garzarolli F., Strasser A., Rudling P. and Wikmark G., *Corrosion of Zirconium Alloys*, ZIRAT7/IZNA2 Special Topics Report, ANT International, Mölnlycke, Sweden, 2002/2003.

Adamson R., Cox B., Davies J., Garzarolli F., Rudling P. and Vaidyanathan S., *Pellet-Cladding Interaction (PCI and PCMI)*, ZIRAT11/IZNA6, Special Topics Report, ANT International, Mölnlycke, Sweden, 2006/2007.

Adamson R., Garzarolli F., Cox B., Strasser A. and Rudling P., *Corrosion Mechanisms in Zirconium Alloys*, ZIRAT12/IZNA7 Special Topics Report, ANT International, Mölnlycke, Sweden, 2007/2008.

Adamson R. B, Garzarolli F., Patterson C., Rudling P. and Strasser A., *ZIRAT14/IZNA9 Annual Report*, ANT International, Mölnlycke, Sweden, 2009.

Adamson R., Garzarolli F., Patterson C., Rudling P., Strasser A., Coleman K. and Lemaignan C., *ZIRAT16/IZNA11 Annual Report*, ANT International, Mölnlycke, Sweden, 2011.

Adamson R., Garzarolli F., Franklin D. and Rudling P., *ZIRAT18/IZNA13 Annual Report*, ANT International, Mölnlycke, Sweden, 2013.

Ade, B., Gauld, I., *Decay Heat Calculations for PWR and BWR Assemblies Fueled with Uranium and Plutonium Mixed Oxide Fuel Using SCALE*, Oak Ridge National Laboratory, Oak Ridge, Tennessee, USA, 2011.

Adkins, H., *Modeling Used Fuel Storage Temperatures*, Nuclear Waste Technical Review Board Meeting, Idaho Falls, Idaho, USA, Pacific Northwest National Laboratory, 2012.

Adkins, H., Geelhood, K., B., K., Coleman, J., Bignell, J., Flores, G., Wang, J.-A., (PNNL), S., Spears, R., Klymyshyn, N., *Used Nuclear Fuel Loading and Structural Performance Under Normal Conditions of Transport – Demonstration of Approach and Results on Used Fuel Performance Characterization*, U.S. Department of Energy, Washington, DC, USA, 2013.

Ahn, T., *Dry Oxidation and Fracture of LWR Spent Fuels*, Division of Waste Management, US Nuclear Regulatory Commission, Washington, DC USA, NUREG-1565, 1996.

Akhiani, H., Szpunar, J., *Effect of Surface Roughness on the Texture and Oxidation Behavior of Zircaloy-4 Cladding Tube*, Applied Surface Science, Vol. 285P, pages 832-839, 2013.

Alvarez, R., Beyea, J., Janberg, K., Kang, J., Lyman, E., Macfarlane, A., Thompson, G., von Hippel, F., *Reducing the Hazards from Stored Spent Power Reactor Fuel in the United States*. Science and Global Security, 11, pp 1-51, 2003.

Copyright © Advanced Nuclear Technology International Europe AB, ANT International, 2014.

Amaya M., Nagase F., Sugiyama T., Udagawa Y., Narukawa T. and Sawada A., *Current Studies at JAEA on Fuel Behaviors under Accident Conditions*, Proceedings of WRFPM 2014, Paper No. 100086 Sendai, Japan, Sep. 14-17, 2014.

Anderson T. and Wilson A., *Ductility of Zircaloy Canning Tubes in Relation to Stress Ratio in Biaxial Testing*, In: Zirconium in the nuclear industry: 4th Int. Symp. ASTM STP-681, J. H. Schemel and T. P. Papazoglou (Eds), American Society for Testing Materials, pp. 60-71, 1979.

Andersson B., *The Enhanced Spacer Shadow Corrosion Phenomenon*, Fachtagung der KTG-Fachgruppe "Brennelemente und Kernbauteile", 29 February/1 March 2000, Forschungszentrum Karlsruhe, 2000.

Andersson B., Limbäck M., Wikmark G., Hauso E., Johnsen T., Ballinger R. G. and Nystrand A-C., *Test Reactor Studies of the Shadow Corrosion Phenomenon*, Zirconium in the Nuclear Industry: 13th Int'l Symposium, ASTM STP 1423, Moan G. D. and Rudling P., Eds., ASTM, 2002.

Andersson T. et al, *Influence of thermal processing and microstructure on the corrosion behaviour of Zircaloy-4 tubing*, IAEA SM 288/59, IAEA, Vienna, 1986.

Andersson T. and Thorvaldsson T., *Nodular corrosion resistance of Zircaloy-2 in relation to second phase particle distribution*, ASTM STP 939, pp. 321-331, 1987.

Anonymous, ASTM Historical Standard G38-73 Standard Practice for making and using C-Ring Stress Corrosion Test Specimens, 1995.

Anonymous, Canadian Standards Association, *Technical Requirements for In-service Evaluation of Zirconium Alloy Pressure Tubes in CANDU Reactors*, Update 2, N285.8-10, 2013a.

Anonymous, ASTM International Standard E1681-03 *Standard Test Method for Determining Threshold Stress Intensity Factor for Environment-Assisted Cracking of Metallic Materials*, Reapproved 2013b.

ANS, *Fukushima Daiichi: ANS Committee Report*, A Report by The American Nuclear Society Special Committee on Fukushima, American Nuclear Society, La Grange Park, Illinois, USA, 2012.

Arimescu I., Goll, W., Hoffmann, P., *Recrystallized Zircaloy-2 Mechanical Properties after Irradiation and Associated Hydrogen Pickup*, TopFuel2013, Charlotte, NC, September, 2013.

Armijo, J. S., Coffin L. F. and Rosenbaum,H. S., *Development of Zirconium-Barrier Fuel Cladding*, Zirconium in the Nuclear Industry., Tenth International Symposium, ASTM STP 1245, Garde A. M., Bradley E. R., (Eds.), American Society for Testing and Materials, West Conshohocken, PA, pp. 3-18, 1994.

Askeljung P., Billone M. and Flanagan M., *Results of integral, high-burnup, fueled LOCA tests and companion testing with as-fabricated and pre-hydrided cladding*. In: IAEA Technical Meeting on Fuel Behavior and Modeling Under Severe Transient and LOCA Conditions, Mito-City, Japan, 2011.

ASTM, *Standard Guide for Drying Behavior of Spent Nuclear Fuel*. American Society for Testing and Materials, Vol. ASTM-1553 08, 2008.

Barberis P, Vauglin C. Fermiot P, and Guerin P., *Thermodynamics of Zr alloys: application to heterogeneous materials*, 17. ASTM Zr Conference, Hyderabad, 2013.

Barraclough K. G. and Beevers C. J., *Some Observations on the Phase Transformations in Zirconium Hydrides*, J. Nucl. Mater., 34, pp. 125-134, 1970.

Copyright © Advanced Nuclear Technology International Europe AB, ANT International, 2014.

Barrow L. et al, *The Zr20Nb–H phase diagram and the characterisation of hydrides in β-Zr2*, J. Nucl. Mat. 442, 292-297, 2013.

Bates D., *Influence of stress state and hydrogen on deformation and failure of Zircaloy-4* (Master of Science), Penn State University, 1998.

Beale J., *Fuel Reliability Update, FRED 4.0*, International Utility Fuel Performance Conference, St. Louis, Missouri, September, 2014.

Beck R. L., *Zirconium-Hydrogen Phase System*, Trans. ASM, 55, pp. 542-555, 1962.

Beie H. J. et al, *Examination of the corrosion mechanism of Zr alloys*, ASTM STP 1245, pp. 615-643, 1994.

Benjamin, A. S., McCloskey D. J., Powers D. A., Dupree S. A., *Spent Fuel Heatup Following Loss of Water During Storage*, Vol. NUREG/CR-0649, US NRC, Washington, DC, USA, 1979.

Bessiron V., Jamet N., Gressier C., Schuh K. D., Sautereau A., Paul T. and Royere C., *AREVA's PCI Methodologies for PWR Enhanced Plant Maneuverability*, Proceedings of WRFPM 2014, Paper No. 100158, Sendai, Japan, Sep. 14-17, 2014.

Bibilashvili Yu K. et al, *Status and development of RBMK fuel rods and reactor materials*, IAEA TECDOC-997, pp. 151-165, 1996.

Bibilashvili Yu K. et al, *Investigation of likely causes of white patch formation on irradiated WWER fuel rod claddings*, IAEA-TECDOC-1128, pp.179-184, 1999.

Bickel G. A., Griffiths M., Chaput H., Buyers A. and Coleman C. E., *Modeling Irradiation Damage in Zr-2.5Nb and its Effects on Delayed Hydride Cracking Growth Rate*, Zirconium in the Nuclear Industry- Seventeenth International Symposium, ASTM STP 1543, 2013.

Billone M., Yan Y., Burtseva T. and Daum R.,.*Cladding Embrittlement During Postulated Loss-of-Coolant Accidents*, NUREG/CR-6967, ANL-07/04, Argonne National Laboratory, Argonne, 2008.

Billone M., Burtseva T., Han Z. and Liu Y., *Embrittlement and DBTT of High-Burnup PWR Fuel Cladding Alloys*, Argonne National Laboratory, Argonne, Illinois, USA, 2013.

Blake E. M., *U.S. Capacity Factors: Still near 90 percent*, Nuclear News, May, 2014.

Blank H., *On the Origin of Different Rates of Inpile Post-transition Oxidation for Zr-based Cladding Alloys*, Z. Metallkunde 85, pp. 645-657, 1985.

Blavius D., Mueuch E-J. and Garner N. L., *Dimensional Behavior of Fuel Channels – Recent Experience and Consequences*, ANS/TOPFUEL, San Francisco, October, 2007.

Boshoven J. and Stoltz M., *Transportation, Aging and Disposal (TAD) NUHOMS® Canisters for Use At the US Repository*, Paper 9493, Paris, France, 2009.

Bouffioux P., Ambard A., Miquet A., Cappelare C., Auzoux Q., Bono M., Rabouille O., Allegre S., Chabretou V. and Scott C. P., *Hydride Reorientation in M5® Cladding and its Impact on Mechanical Properties*, Top Fuel 2013, Charlotte, North Carolina, USA, American Nuclear Society, 2013.

Brach E. W., *Cladding Consideration for the Transportation and Storage of Spent Fuel*, USNRC Interim Staff Guidance – 11, Revision 3, Spent Fuel Project Office, 2003.

BRC, *Reactor and Fuel Cycle Technology Subcommittee, Report to the Full Commission, Updated Report*, Blue Ribbon Commission on America's Nuclear Future, Washington, DC, USA, 2012a.

Copyright © Advanced Nuclear Technology International Europe AB, ANT International, 2014.

BRC, *Transportation and Storage Subcommittee Report to the Full Commission, Updated Report*, Blue Ribbon Commission on America's Nuclear Future, Washington, DC, USA, 2012b.

Broy Y., Garzarolli F., Seibold A. and Van Swam L. F., *Influence of transition elements Fe, Cr, and V on long time corrosion in PWRs*, Zirconium in the Nuclear Industry: 12th Int'l Symposium, ASTM STP 1354, pp. 609-622, G. P. Sabol and G. D. Moan, Eds., West Conshohocken, PA, 2000.

Bruemmer G. et al, *Labor- und Bestrahlundsversuche an Hüllrohren mit reduzierter Neigung zur nodularen Korrosion*, Jahrestagung Kerntechnik, Karlsruhe, Germany, 1987.

Bruemmer G. et al, *Optimierung der Hüllrohre für Siedewasserreaktoren,* Jahrestagung Kerntechnik, Köln, Germany, 1992.

Bunn M., et al, *Interim Storage of Spent Nuclear Fuel, A Safe, Flexible, and Cost-Effective Near-Term Approach to Spent Fuel Management*, A Joint Report from the Harvard University Project on Managing the Atom and the University of Tokyo Project on Sociotechnics of Nuclear Energy, Cambridge, MA, USA, 2001.

Burr P. A. et al, *Hydrogen solubility in zirconium intermetallic second phase particles*, J. Nucl. Mat. 443, 502-506, 2013.

Cantonwine P., Paustian H., Hahn G. and Tusar J., *Channel – Control Blade Interference in GE Boiling Water Reactor, D-Lattice Plants with Zircaloy-2 Channels*, Michael Reitmeyerd, and Erik Madere, LWR Fuel Performance Meeting/TopFuel/WRFPM, Paper 079, Orlando, Florida, USA, September 26-29, 2010.

Capps N., Montgomery R., Sunderland D., Spencer B., Pytel M. and Wirth B. D., *Evaluation of Missing Pellet Surface Geometry on Cladding Stress Distribution and Magnitude*, Proceedings of WRFPM 2014, Paper No. 100109, Sendai, Japan, Sep. 14-17, 2014.

Carter J. T., Jones R. H. and Luptak A. J., *U.S. Radioactive Waste Inventory and Characteristics Related to Potential Future Nuclear Energy Systems*, Vol FCRD-USED-2011-000068, Rev 2, U.S. Department of Energy, Used Fuel Disposition, Washington, D.C., USA, 2011.

Carter J. T., Luptak A. J., Gastelum J., Stockman C. and Miller A., *Fuel Cycle Potential Waste Inventory for Disposition*, Savannah River National Laboratory, Savannah, Georgia, USA, 2012.

Cazalis B., Bernaudat C., Yvon P., Desquines J., Poussard C. and Averty X., *The Prometra Program: A Reliable Material Database for Highly Irradiated Zircaloy-4™ and M5™ Fuel Claddings*, Proc. 18th International Conference on Structural Mechanics in Reactor Technology, SMiRT 18-C02-1, Beijing, China, August 7-12, 2005.

Chapin D., Brashier R., Staub D., O'Cain M., Höglund J., Jasiulevicius A.,Joseffson B., Andersson T., Oehman A., *Design and Operation of EFG Fuel in Ringhals PWRs*, TopFuel 2013, Charlotte, NC, September, 2013.

Châtelain A., Anderson B., Ballinger R. G. and Wikmark G., *Enhanced Corrosion of Zirconium Base Alloys in Proximity to Other Metals: the Shadow Effect*, p.485-498, Int. Topical Meeting on LWR Fuel Performance, Park City, UT, April, 2000.

Chen J. S. F. and Adamson R. B., *Observations of Shadow Phenomena on Zirconium Alloys*, Proceedings of the International Topical Meeting on LWR Fuel Performance, ANS, West Palm Beach, Florida, 309-317, 1994.

Cheng B. and Adamson R. B., *Mechanistic Studies of Zircaloy Nodular Corrosion*, ASTM STP 939, pp. 387-416, 1987.

Copyright © Advanced Nuclear Technology International Europe AB, ANT International, 2014.

Cheng B. et al, *Corrosion performance of some Zirconium alloys irradiated in the SGHWR Winfrith*, 1st Environmental Degradation Conference, Myrtle Beach, USA, 1983.

Cheng B. et al, *Development of a Sensitive and Reproducible Steam Test for Zircaloy Nodular Corrosion*, ASTM STP 939, pp. 257-283, 1987.

Cheng B., Oberlander B. C., Wiesenack W., Yagnik S. and Turnbull J., *An In-reactor Simulation Test to Evaluate Root Cause of Secondary Degradation of Defective BWR Fuel Rod,* Zirconium in the Nuclear Industry., Thirteenth International Symposium, ASTM STP 1423, Moan, G.D., Rudling, P., (Eds.), American Society for Testing and Materials, West Conshohocken, PA, pp. 616-633, 2002.

Chernishov V. and Troyanov V., *Lessons Learned from Control Rods Irradiation Experience, Development of Advanced Absorbers and their Refractory properties Under Accident Conditions*, ANS International Topical Meeting on LWR Fuel performance, Portland, Oregon, Kap. 10March, 1997.

Chiu W-J., Cheng S-C., Shiu Y-H. and Tseng C-C., *Results of Post-Irradiation Examinations for BWR Failure Rods*, Proceedings of Top Fuel 2009, Paris, France, September 6-10, 2009.

ChiuW., Cheng S. and Shiu, Y., *The HWC Fuel Surveillance of BWR-6 NPP in Taiwan*, WRFPM 2014, Sendai, Japan, 2014.

Chopra O., Diercks D., Ma D., Shah V., Tam S-W., Fabian R., Han Z. and Liu Y., *Managing Aging Effects on Dry Cask Storage Systems for Extended Long-Term Storage and Transportation of Used Fuel, Rev. 1*, Argonne National Laboratory, Argonne, Illinois, USA, 2013.

Choudhuri G. et al, *Influence of Fe content on corrosion and hydrogen pick up behavior of Zr–2.5Nb pressure tube material*, J. Nucl. Materials 441, pp. 178-189, 2013.

Christensen M. et al, *Effect of alloying elements on the properties of Zr and the Zr–H system*, J. Nucl. Mat. 445, 241-250, 2014.

Chung H. M. and Kassner T. F., *Cladding metallurgy and fracture behavior during reactivity-initiated accidents at high burnup*, Nucl. Eng. Design, 186, pp. 411-427, 1998.

Clifford P., *The US Nuclear Regulatory Commission's Strategy for Revising the RIA Acceptance Criteria,* Int. LWR Fuel Performance Meeting, San Francisco, CA, September, 2007.

Cohen M., *Interim Storage of Used Nuclear Fuel*, NEI Dry Storage Information Forum, Tarpon Springs, FL, USA, 2009.

Cole S. E., Garner N. L., Lippert H. –J., Graebert R., Mollard P. and Hahn G. C., *Protecting AREVA ATRIUM BWR Fuel from Debris Fretting Failure*, Proceedings of WRFPM 2014, Paper No. 100164, Sendai, Japan, Sep. 14-17, 2014.

Cole S. E., Garner N. L., Lippert H-J., Graebert R., Mollard P. and Hahn G. H., *Protecting AREVA ATRIUM™ BWR Fuel from Debris Fretting Failure,* Water Reactor Fuel Performance Meeting 2014, Sendai, Japan, Paper 100164.

Coleman C. E., *Simulation of interaction between cracked UO_2 fuel and Zircaloy cladding,* Proc. International Conference on Physical Metallurgy of Reactor Fuel Elements, The Metals Soc., London UK., pp.302-307, 1974.

Coleman C. E., Doubt G. L., Fong R. W. L., Root J. H., Bowden J. W., Sagat S. and Webster R. T., *Mitigation of Harmful Effects of Welds in Zirconium Alloy Components*, Zirconium in the Nuclear Industry: Tenth International Symposium, ASTM STP 1245, Garde A. M., Bradley E. R., Eds., American Society for Testing and Materials, Philadelphia, pp. 264-284, 1994.

Copyright © Advanced Nuclear Technology International Europe AB, ANT International, 2014.